Diplomarbeit zur Erlangung des akademischen Grades
Diplomingenieur der Lebensmittel und Biotechnologie

Getting insights into the interaction of WRN and SNEV$^{Prp19/Pso4}$

betreut von
Priv. Dozent Dipl.-Ing. Dr. Johannes Grillari
Univ. Ass. Dipl.-Ing. Dr. Regina Voglauer

Durchgeführt am Institut für Angewandte Mikrobiologie
der Universität für Bodenkultur Wien

Eingereicht von Martina Strauss
Wien, März 2007

Index

1 Abstract

We have identified SNEVPrp19/Pso4 as a protein that is downregulated in various senescent cells, when compared to early passage or immortalized cells. Interestingly, overexpression of SNEVPrp19/Pso4 in human umbilical vein endothelial cells leads to an increased replicative life span of the cells in vitro. Additionally, SNEVPrp19/Pso4 has been found as a member of the CDC5L complex, where it plays an essential role in pre-mRNA splicing as well.

Furthermore, it has recently been shown that 4 proteins of the CDC5L complex are physically interacting with Werner protein (WRN), while repairing inter strand cross links (ICLs). Like SNEVPrp19/Pso4, WRN seems to play an essential role in cellular aging as well, since mutations induce a segmental progeroid disease, the Werner syndrome, where patients show a premature aging phenotype.

The aim of this study was to get a deeper insight into the possible interaction between WRN and SNEVPrp19/Pso4, especially the role of these proteins in stress resistance and DNA damage repair after treatment of cells with substances inducing oxidative or genotoxic stresses. Furthermore, splicing assays were performed in order to test whether WRN is involved in the splicing machinery as well.

2 Introduction

2.1 Senescence

In 1961 Leonard Hayflick and Paul Moorhead discovered that human cells derived from embryonic tissues can only divide a finite number of times in culture before entering the phase of replicative senescence (Hayflick and Moorhead 1961). This finding overturned the hypothesis, set up by Alexis Carrel in 1912, that single cells once removed from the organism are able to live infinite.

Although senescent cells remain metabolically active, they enter a phase of growth arrest, which is irreversible and replication cannot be reactivated by physiologic mitogens. Senescent cells in many aspects resemble terminally differentiated cells (Goldstein 1990). Additionally, senescence seems to stabilize the cell, providing greater resistance to programmed cell death (apoptosis) (Wang 1995).

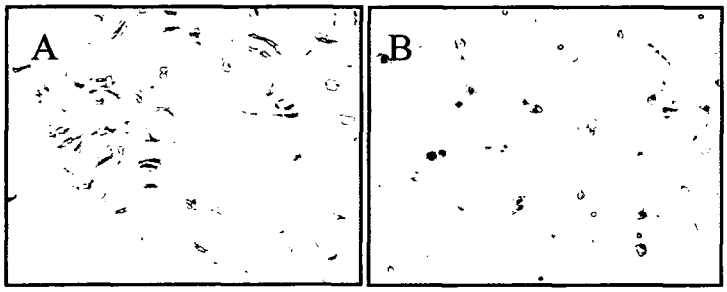

Fig.1: β-galactosidase stained young (A) and senescent (B) HUVECs (Voglauer, Chang, Dampier, Wieser, Baumann, et al. 2006)

Senescence in culture can be recognised by several morphological and biochemical changes, such as a flatten and enlarged morphology and polynuclear cells as well as the expression of β-galactosidase, exhibiting a common marker for cellular senescence (Dimri, Lee, Basile, Acosta, Scott, et al. 1995). Fig.1 shows the morphology of early passaged and senescent HUVECs (human umbilican vein endothelial cells) with a positive stain for β-galactosidase in senescent cells.

But what are the causes for senescence?

2.1.1 Telomere dependent senescence

In 1973, Olovnikov proposed that the induction of replicative senescence originates from telomere shortening to a critical extend (Olovnikov 1973). The telomeres, tandem repeats of the DNA sequence TTAGGG with a 3' overhang, cap the ends of chromosomes thereby protecting the chromosomes from degradation (Blackburn 2005). These telomeres normally form a loop structure, named t-Loop (Griffith, Comeau, Rosenfield, Stansel, Bianchi, et al. 1999). In this structure, the telomere turns back and the single strand forms a loop by inserting into the double helix as seen in Fig. 2. TRFs (telomere repeat-binding factors) are found to bind and thereby stabilize the telomeric loop structure. One of these proteins TRF1 is binding to the double-strand by recognizing the specific telomeric DNA sequence. TRF2 binds at the junction between the double and single stranded areas of DNA, allowing the single-stranded end of the telomere to be folded-back and completely buried within the double stranded region. (Fig. 2)

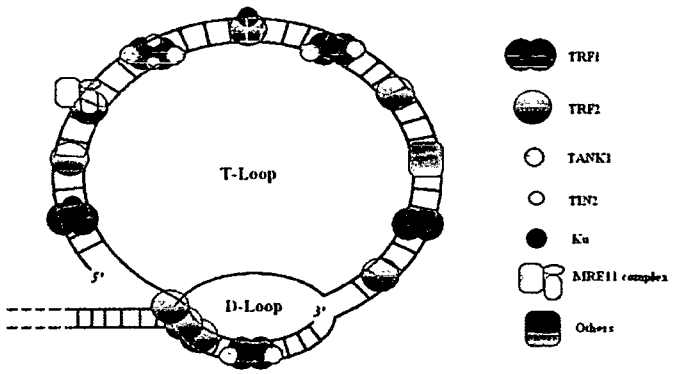

Fig. 2: A view of telomere structure, the T-Loop associated with telomere-binding proteins (Lin Kah Wai et al 2004)

The loss of TRF2 leads to a collapse of the t-Loop structure in vitro. The inhibition of TRF2 binding in vivo triggers apoptosis, mediated by p53 and the ATM kinase, leading to cell death, suggesting an essential role of the t-Loop in genomic stability and cell survival (Karlseder, Broccoli, Dai, Hardy, and de Lange 1999).

In each round of replication the telomeres shorten, due to the inability of the DNA replication machinery to completely replicate the very ends of the chromosomes [the "End replication

problem" (Olovnikov 1973)]. Once the telomeres have reached a critically short length, they aren't able to form a loop with itself anymore and replicative senescence or apoptosis, depending on cell type, is triggered (Beausejour, Krtolica, Galimi, Narita, Lowe, et al. 2003; Harrington and Robinson 2002). The telomeres are therefore called the cell's clock that possesses a counting mechanism, determining the replicative life span of cells (Harley 1991). Although the mechanisms with which telomeres are triggering senescence is yet poorly understood, it is thought that telomere dysfunction evoke DNA damage responses, similar to those triggered by ds (double strand) breaks (d'Adda di Fagagna, Reaper, Clay-Farrace, Fiegler, Carr, et al. 2003). Only actively dividing cells such as most cancer cells as well as embryonic stem cells have gained mechanisms to prevent progressive telomere erosion and to maintain the telomeres at a stable length. The enzyme responsible for the elongation of the telomeric repeat sequences, the telomerase, was first discovered by Blackburn and Greider (Greider and Blackburn 1985). Telomerase is a holoenzyme consisting of the catalytic subunit hTERT and a RNA component. Inhibition of telomerase activity in tumour cells leads to progressive telomere shortening and subsequently resulting in cell death (Hahn, Stewart, Brooks, York, Eaton, et al. 1999). On the other hand the overexpression of hTERT is sufficient to immortalise various human normal cells (Bodnar, Ouellette, Frolkis, Holt, Chiu, et al. 1998; Chang, Grillari, Mayrhofer, Fortschegger, Allmaier, et al. 2005; Rufer, Migliaccio, Antonchuk, Humphries, Roosnek, et al. 2001; Zhang, Mar, Zhou, Harrington, and Robinson 1999). For the immortalisation of some cell lines, e.g. mammary epithelial cells and keratinocytes, however, additional inhibition of $p16^{INK4A}$ tumour suppressor protein seems to be essential (Dickson, Hahn, Ino, Ronfard, Wu, et al. 2000; Kiyono, Foster, Koop, McDougall, Galloway, et al. 1998). Whether this results from inadequate culture conditions is a matter of lively debate.

Quite surprising findings suggest that the telomerase as a protein is not only involved in the maintenance of the telomere length but also in the telomere capping itself (Blackburn 2005). Introduction of hTERT in precrisis fibroblast leads to an immortalisation of the cells, although telomeres had already shortened beyond the critical length of telomere maintenance (Zhu, Wang, Bishop, and Blackburn 1999).

2.1.2 Telomere independent senescence

Besides telomere dependent senescence as described previously other mechanisms have been found that lead to senescence like phenotypes.

The expression of certain oncogenes such as oncogenic Ras results in a permanent growth arrest while accumulating p53 and p16 (Serrano, Lin, McCurrach, Beach, and Lowe 1997). Furthermore, DNA damage, caused by radiation, leads to a p53-dependent G1 arrest resembling replicative senescence in normal human diploid fibroblasts (Di Leonardo, Linke, Clarkin, and Wahl 1994). Additionally, it has been found that treatment with subletal doses of oxidants may result in "stress induced premature senescence" (Toussaint, Dumont, Remacle, Dierick, Pascal, et al. 2002). Cultivation of human diploid fibroblasts in vitro under physiological oxygen conditions significantly extends the lifespan for about 20 population doublings (Chen, Fischer, Reagan, Yan, and Ames 1995). Whereas concentrations higher than the atmospheric oxygen concentration accelerate growth arrest in human melanocytes (Horikoshi, Balin, and Carter 1991).

.

2.1.3 Cellular senescence and aging

The fact that the replicative live span of cells correlates with the age and the longelevity of the donor species proposes a linkage between cellular senescence and organismic aging (Cristofalo and Pignolo 1993; Stanulis-Praeger 1987). An evidence for this suggestion is that cellular senescence and organismic aging also share physiologic and molecular features. The stress inducibility, for example of heat shock protein 70 is markedly attenuated in senescent human fibroblasts (Choi, Lin, Li, and Liu 1990) and several tissues from aged rodents (Heydari, Wu, Takahashi, Strong, and Richardson 1993). This effect results through a reduced binding of a heat shock transcription factor.

Additionally, in human skin tissues the activity of SA (senescence associated) β-galactosidase increases with the age of skin cells (Dimri, Lee, Basile, Acosta, Scott, et al. 1995). This phenomenon is not associated with quiescence, terminal differentiation, or immortality, which provide in situ evidence that senescent cells do in fact accumulate in aged tissues in *vivo*. Other astonishing findings indicate an involvement of senescent cells in age associated

diseases such as atherosclerosis and cardiovascular diseases (Erusalimsky and Kurz 2005; Minamino and Komuro 2007). Cells derived from patients suffering from progeriod diseases such as the WS (Werner syndrome) undergo premature senescence. This phenomenon confirms that senescence is not an in *vitro* artefact (Allsopp, Vaziri, Patterson, Goldstein, Younglai, et al. 1992).

What could be the in vivo relevance of senescence?

The permanent growth arrest of cells in *vivo* impairs the self-renewal potential of organs (Satyanarayana, Wiemann, Buer, Lauber, Dittmar, et al. 2003). However, the altered functions of senescent cells may have a substantial impact in aged tissue as well. Senescent human skin fibroblasts overexpress collagenase and underexpress collagenase inhibitors which could likely cause the collagen breakdown, evoking the thin dermis as seen in old people's skin (West, Pereira-Smith, and Smith 1989).

Defence mechanism against cancer development has been proposed as a main role for senescence in vivo, suggesting that growth arrest besides apoptosis is another possibility to prevent tumour development (Rodier, Kim, Nijjar, Yaswen, and Campisi 2005). Contradictory to the tumour suppression function of cellular senescence, senescent human fibroblasts have been observed to stimulate tumorigenesis in premalignat epithelial cells and to alter the morphological and functional differentiation of mammary gland cells (Krtolica, Parrinello, Lockett, Desprez, and Campisi 2001; Parrinello, Coppe, Krtolica, and Campisi 2005). These results suggest a role of senescent cells in aged organism by evoking cancer. Evolutionary aspects underline these statements, suggesting that some genes, selected to enhance the fitness of young organisms, can have unspecific deleterious effects in aged organisms.

2.2 SNEV

Since cellular physiology and phenotype are determined by the repertoire of expressed and translated genes it is of utmost importance to find proteins involved in cellular senescence and aging. SNEV has been identified in our lab as a protein downregulated in replicative senescent HUVECs when compared to early passaged cells (Grillari, Hohenwarter, Grabherr, and Katinger 2000). SNEV is an ubiquitinously expressed, highly conserved protein, which seems to play an important role in many different cellular processes such as splicing, DNA repair, stress resistance and ubiquitination (Grillari 2007). The sequence of SNEV displays high homology from yeast to humans. Highest homology can be seen at the N-terminus, whereas the C-terminus differs in sequence, but not in domain architecture (Fig. 3).

Synonyms for SNEV are: (SNEV [Senescence Evasion Factor], hPRP19 [human pre-mRNA processing 19], hPSO4 [human psoralen sensitivity 4], hNMP200 [human nuclear matrix protein 200]). In the following the generalized term, SNEV$^{Prp19/Pso4}$ is used.

Fig. 3: Sequence comparison of *S. cerevisiae*, *C. elegans*, and human SNEV$^{Prp19/Pso4}$. Homology of SNEV$^{Prp19/Pso4}$ and Prp19 by sequence comparison (BLAST database) revealed 23% (104/439) identities, and 41% (184/439) positives, the last 81 (SNEV$^{Prp19/Pso4}$), respectively 99 (Prp19) aa were not matched. Homology of SNEV$^{Prp19/Pso4}$ and T10F2.4 revealed 50% (253/505) identities, and 67% (340/505) positives, the first 17 aa of T10F2.4 did not match. (Grillari 2007)

As shown in Fig. 4 the protein SNEV$^{Prp19/Pso4}$ consists of a U-box (E3-Ligase activity), a coiled-coiled region (self interaction), a low complexity region and 7WD40 repeats.

Fig. 4: Putative functional domains of SNEV $^{Prp19/Pso4}$

In the following the multifunctional properties of SNEV$^{Prp19/Pso4}$ are described.

2.2.1 SNEV$^{Prp19/Pso4}$ is involved in ubiquitination

As mentioned above SNEV$^{Prp19/Pso4}$ consists of 4 structural motifs, one of them, the U-box, has been identified as a putative E3 ligase domain (Aravind and Koonin 2000). Although the E3 ligase activity of SNEV$^{Prp19/Pso4}$ has been proven, its ubiquitination substrate remains unknown. In cooperation with the E2 ligase UbcH3 and an E1 enzyme, SNEV$^{Prp19/Pso4}$ is able to form poly ubiquitin chains (Hatakeyama, Yada, Matsumoto, Ishida, and Nakayama 2001). The U-box domain of SNEV$^{Prp19/Pso4}$ has been found to physically interact with the proteasome (PSMB4) without being degraded (Loscher, Fortschegger, Ritter, Wostry, Voglauer, et al. 2005). Since inhibition of the proteasome leads to an increased colocalisation of SNEV$^{Prp19/Pso4}$ with the proteasome and with ubiquitin, SNEV$^{Prp19/Pso4}$ is suggested to be a vehicle, that conducts target proteins to the proteasome for degradation (Loscher, Fortschegger, Ritter, Wostry, Voglauer, et al. 2005). In yeast, the E3 ligase activity has been verified as well, and a deletion of the U-box has been found to block ubiquitination in *vitro* and is lethal in *vivo* as shown by plasmid shuffling assays (Ohi, Vander Kooi, Rosenberg, Chazin, and Gould 2003).

2.2.2 SNEV$^{Prp19/Pso4}$ extends the replicative life span of HUVEC

Overexpression of SNEV$^{Prp19/Pso4}$ leads to an extended life span in HUVECs (Voglauer, Chang, Dampier, Wieser, Baumann, et al. 2006). This effect is not due to altered telomerase

activity or telomere dynamics, but rather due to enhanced stress resistance. After treatment of the cells with bleomycin or bleomycin combined with buthionine sulfoximine (BSO), substancese that are generating reactive oxygen species (ROS) and DNA damage, SNEV$^{Prp19/Pso4}$ overexpressing cells show a higher survival and a lower amount of apoptotic cells (Voglauer, Chang, Dampier, Wieser, Baumann, et al. 2006).

2.2.3 SNEV$^{Prp19/Pso4}$ is a pre-mRNA splicing factor

By screening temperature sensitive yeast mutants, showing defects in splicing, a 504 aa large protein has been identified as an essential factor for pre-mRNA splicing, named prp19 (Cheng, Tarn, Tsao, and Abelson 1993), the yeast homologue of SNEV$^{Prp19/Pso4}$. In a proteomic approach, combining mass spectrometry and EST-database search, SNEV$^{Prp19/Pso4}$ has been found as a putative member of the spliceosome machinery as well (Neubauer, King, Rappsilber, Calvio, Watson, et al. 1998). Together with CDC5L, the human ortholoque of yeast CDC5, SNEV$^{Prp19/Pso4}$ has been found to build up a protein complex, named CDC5L complex (Ajuh, Kuster, Panov, Zomerdijk, Mann, et al. 2000). This complex is highly conserved in yeast and interacts with the spliceosome (Tarn, Lee, and Cheng 1993) required for the second catalytic step of pre-mRNA splicing (Fig. 5).

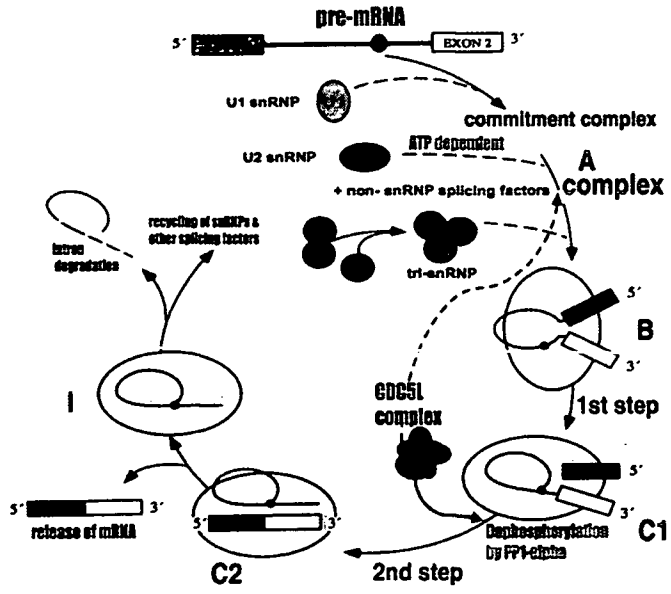

Fig. 5: The role of the CDC5L complex in the splicing machinery

Immunodepletion of the CDC5L complex inhibits the formation of pre-mRNA splicing products in vitro but does not prevent spliceosome assembly (Ajuh, Kuster, Panov, Zomerdijk, Mann, et al. 2000). However, some results suggest a role of SNEV$^{Prp19/Pso4}$ prior to catalysis. SNEV$^{Prp19/Pso4}$ has been found in the B* complex (Makarov, Makarova, Urlaub, Gentzel, Will, et al. 2002) as well as in the BΔU1 complex (Makarova, Makarov, Urlaub, Will, Gentzel, et al. 2004) and the B complex (Deckert, Hartmuth, Boehringer, Behzadnia, Will, et al. 2006). In addition, our protein-protein interaction assays are providing evidence that SNEV$^{Prp19/Pso4}$ is interacting with itself by the amino acids sequence region 56-74. Furthermore, inhibition of the self interaction using synthetic peptides from the self interaction region is leading to a destabilisation of the spliceosome complex, suggesting an essential role of SNEV$^{Prp19/Pso4}$ in assembly of the spliceosome (Grillari, Ajuh, Stadler, Loscher, Voglauer, et al. 2005).

2.2.4 SNEV$^{Prp19/Pso4}$ knock out is lethal to mouse embryos

Depletion of SNEV$^{Prp19/Pso4}$ and its homoloques in different model organisms suggests an essential role in the maintenance and development of the early embryonic organisms. Knock-down (KD) in *C. elegans* (Gonczy, Echeverri, Oegema, Coulson, Jones, et al. 2000), *D. melanogaster* (Milchanowski, Henkenius, Narayanan, Hartenstein, and Banerjee 2004) or in *S. cerevisiae* (Giaever, Chu, Ni, Connelly, Riles, et al. 2002) have shown to be lethal. Recent studies in our lab showed that mice with a homozygous KD of SNEV$^{Prp19/Pso4}$ are not viable and die during early embryonic development (Fortschegger, Wagner, Voglauer, Katinger, Sibilia, et al. 2007). In contrast heterozygous mutants can develop and yet don't show crucial abnormalities in development and morphology. However when culturing mouse embryonic fibroblasts from a pregnant female (+/-) KD mouse, they show a decreased growth potential in *vitro*.

2.2.5 SNEV$^{Prp19/Pso4}$ is involved in DNA repair

SNEV$^{Prp19/Pso4}$ has been identified as a protein, interacting with TdT (terminal deoxynucleotidyl transferase) an enzyme involved in the repair of ds breaks and SNEV$^{Prp19/Pso4}$ expression level can be enhanced by γ radiation and chemical mutagens. The depletion of SNEV$^{Prp19/Pso4}$ by siRNA leads to an accumulation of ds breaks, apoptosis, and decreased cell survival after DNA damage, suggesting SNEV$^{Prp19/Pso4}$ to play an important role in the repair of double strand breaks (Mahajan and Mitchell 2003).

Additionally, recent studies have shown that SNEV$^{Prp19/Pso4}$ and CDC5L, PLRG1, and SPF27, three components of the CDC5L associated complex are interacting with WRN protein during early steps of DNA interstrand cross link repair (Zhang, Kaur, Lu, Shen, Li, et al. 2005).

2.3 WRN

2.3.1 WRN deficiency syndrome (WS)

The characteristics of human Werner syndrome (WS), originally defined by Otto Werner in 1904, resemble in many ways an acceleration of normal aging (Salk 1982). WS patients are fairly asymptomatic early in life but they prematurely develop many, but not all, phenotypic changes correlated with age. Additional to the physical appearance such as wrinkled, thinning skin and greying hair (Fig. 6). WS patients suffer from typical age-related diseases like arteriosclerosis, type II diabetes, bilateral cataracts, osteoporosis, and thymic atrophy (Martin 1999). The most common cause of death for WS patients is cancer and coronary heart diseases at an average age of 47 years.

Fig. 6: Phenotypic chances correlated with Werner disease; Japanese girl as a teenager (left) and by the age of 48 (right) [William and Wilkens Publishing Inc.]

2.3.2 WRN protein

WRN protein is located on chromosome 8p11-p12 (Oshima, Yu, Boehnke, Weber, Edelhoff, et al. 1994) and mutations leading to nonfunctional protein are responsible for the clinical out come of WS (Yu, Oshima, Fu, Wijsman, Hisama, et al. 1996).WRN is a member of the RecQ family of DNA helicases and possesses 3'–5' exonuclease activity in addition to 3'–5' helicase activity (Harrigan and Bohr 2003) (Fig. 7). Neither the yeast nor bacterial RecQ helicases possess exonuclease activity, which makes this protein quite unique. Since the 35EXOc (exonuclease domain) at the N-terminus of WRN is homologous to the proofreading domain of E.coli's DNA polymerase I, which works by the hydrolysis of unpaired or mismatched nucleotides (Foreman and Hamlin 1989; Mushegian, Bassett, Boguski, Bork, and Koonin 1997) WRN has been proposed to function as an autonomous proofreading enzyme as well.

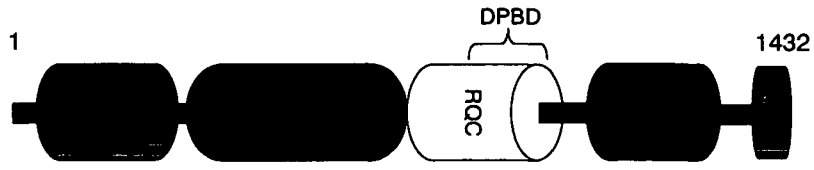

Fig.7: Structural domains of WRN protein: Nuclease (35EXOc domain responsible for the 3'-5' exonuclease proofreading activity of DNA polymerase I in E.coli), Helicase (DEXH-box helicase: domain of a diverse family of proteins involved in ATP-dependent DNA or RNA unwinding), RecQ-helicase (HELICc: domain found in a wide variety of helicases and helicase related proteins) and HRDC (Helicase and RNase D C-terminal domain has a putative role in nucleic acid binding) The DPBD (DNA and Protein binding Domain) is the major site for structure specific DNA and functional protein binding
[www.ncb.gov]

2.3.2.1 WRN and replication

As WS cells show reduced growth potential in *vitro*, WRN has been supposed to play an essential role in replication. The majority of cells derived from WS patients stop proliferation in G1 phase and the progression of S-phase seems to be delayed (Fujiwara, Higashikawa, and Tatsumi 1977; Poot, Hoehn, Runger, and Martin 1992). This effect is probably due to WRN's helicase activity that is capable of unwinding various DNA structures, like D-loops and G-quartets, structures potentially associated with the progression of the replicative fork (Rodriguez-Lopez, Jackson, Iborra, and Cox 2002). Additionally, the 144 aa RecQ DNA helicase domain of WRN has been shown to extensively stimulate the rate of FEN-1, a DNA structure-specific nuclease supposed to be involved in the processing of Okazaki fragments, by direct protein interaction as well (Brosh, von Kobbe, Sommers, Karmakar, Opresko, et al. 2001). Furthermore WRN and chromatin assembly factor 1 (CAF-1), involved in the maintenance of genomic stability, relocate to sites where DNA synthesis takes place when treated with DNA-damaging substances (Jiao R 2006).

2.3.2.2 WRN protects non proliferating cells from oxidative stress

A down regulation of WRN leads to an accelerated cellular senescence phenotype and DNA damage response in normal fibroblasts shown by induction of γH2AX and 53BP1 nuclear foci

(Szekely, Bleichert, Numann, Van Komen, Manasanch, et al. 2005). These nuclear damage foci are prominently present in non dividing cells. Cultivating WRN depleted cells in physiological (3%) oxygen or in the presence of an antioxidant prevents the development of the DNA damage foci in WRN-depleted cells, whereas acute oxidative stress leads to inefficient repair of the lesions (Szekely, Bleichert, Numann, Van Komen, Manasanch, et al. 2005). The observation, that rapidly dividing cells (such as those found in the bone marrow and intestinal epithelium) derived from Werner syndrome patients display a relatively normal appearance, could be explained by a repair mechanisms activated during replication. These mechanisms might actually repair the lesions, accumulated in G_1 phase in WRN-deficient cells. Defects in DNA replication and development of chromosomal abnormalities in cells derived from Werner syndrome patients might display a secondary consequence of the inability to repair DNA lesions accumulated during prolonged G_1 phase.

2.3.2.3 WRN and DNA repair

WRN has been shown recently to physically interact with Ku 86/70 proteins that are involved in the repair of dsbreaks formed by V(D)J joining, or as a result of ROS, ionization radiation or chemotherapeutic drugs. The Ku 86/70 is thereby stimulating WRN's exonuclease activity, suggesting their participation in a common DNA metabolic pathway (Cooper, Machwe, Orren, Brosh, Ramsden, et al. 2000).

Very recent studies have proposed a role for WRN in telomere-based DNA damage responses as well. When telomeres shorten to a critical level, cells are entering replicative senescence, whereby uncapped telomere overhangs can be recognised as DNA breaks. WRN has been demonstrated to play a role in processing telomeric DNA by activating DNA damage responses. After treatment with t-oligos, which mimic uncapped telomere overhangs, WRN KD cells show reduced phosphorylation of p53 and histone H2AX (Eller, Liao, Liu, Hanna, Backvall, et al. 2006)

Recently WRN has also been found to play a role in BER (base excision repair) in *vivo* where it cooperates through its helicase and exonuclease activities with poly β, while processing BER. In addition, stable WRN/KD cell lines show an increased sensitivity to the methylating

agent methyl methanesulfonate (MMS) and extracts from WRN/KD cells displayed reduced LP (long patch) BER activities (Harrigan JA 2006).

2.3.2.4 WRN and ICLs

DNA interstrand cross-links (ICLs) are toxic lesions that block DNA replication inhibiting mitosis. Therefore, ICLs inducing agents have been widely used for cancer chemotherapy. Repair of DNA ICLs involves homologous recombination (HR) and nucleotide excision repair (NER). A recent study demonstrates that WRN and BRCA1 physically interact while processing DNA ICLs. The cell seems to require both, BRCA1 and the helicase activity of WRN (Cheng, Kusumoto, Opresko, Sui, Huang, et al. 2006). Another result confirm WRNs role in the repair of ICLs. Following the induction of ICL, WRN has been found to relocate from nucleoli to arrested replication forks in the nucleoplasm, where it interacts with the HR protein Rad52 (Otterlei, Bruheim, Ahn, Bussen, Karmakar, et al. 2006).

3 The aims

Previous reports have shown that WRN and SNEV$^{Prp19/Pso4}$ interact physically while processing ICLs, thus playing an important role in DNA damage repair. This function might lay the ground for the involvement of these proteins in cellular aging in *vitro* and in *vivo*.
Aim of the following study was to get a deeper insight into the involvement of WRN and SNEV$^{Prp19/Pso4}$ in DNA damage repair especially after treatment with genotoxic substances. Furthermore, since SNEV$^{Prp19/Pso4}$ has been demonstrated to be an essential splicing factor, we also wanted to test whether WRN is also involved in the splicing reaction.

Therefore, the following working packages were conducted:

Deletion mutants of SNEV$^{Prp19/Pso4}$ should be cloned, aiming to define the interaction domain between WRN and SNEV$^{Prp19/Pso4}$

WRN/KD cell line should be characterized in order to find out how WRN depletion affects growth and morphology.

A stressing protocol for WRN/KD cells should be set up in order to confirm WRNs function in repair processes.

HeLa cells should be depleted from both proteins WRN and SNEV$^{Prp19/Pso4}$, followed by treatment with Cisplatin in order to get deeper insights into the role of these two proteins in DNA damage repair.

A splicing assay should be established in order to determine whether WRN exhibits a possible role in splicing as well.

4 Materials and Methods

For recipes of buffer and solutions and sequences see Appendix

4.1 Plasmids and siRNAs

4.1.1 PCI neo

The pCI-neo mammalian expression vector carries the human cytomegalovirus (CMV) as promoter ensuring a strong constitutive expression of cloned DNA inserts in mammalian cells. The pCI-neo vector contains an ampilicin resistance and the neomycin phosphotransferase gene (Fig. 8). The pCI-neo vector can be used for transient or for stable expression in mammalian cells by selecting transfected cells with the antibiotic G418.

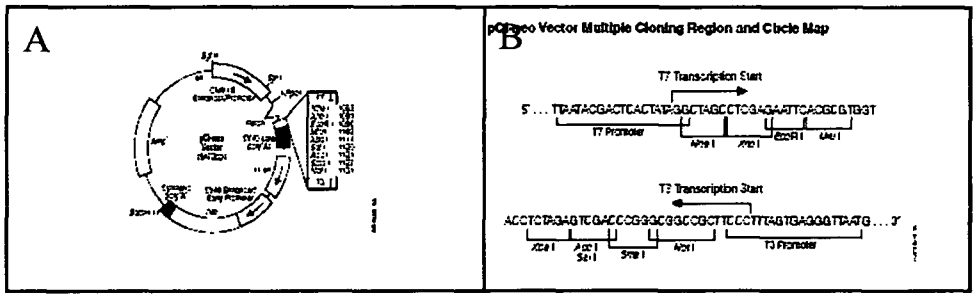

Fig. 8: (A) pCI-neo vector circle map (Neo=neomycin;CMV=cytomegalovirus) (B) multiple cloning site (MCS) sequence of the pCI-neo vector.
[Taken from Invitrogen cataloque]

4.1.2 pEGFP-C1

The pEGFP-C1 vector encodes a red-shifted, brighter fluorescing, variant of wild-type GFP (Excitation max. = 488 nm; emission max. = 507 nm.) The vector contains an SV40 promotor for replication in mammalian cells, neomycin/kanamycin resistance and poly A signals from thymidine kinase (Fig. 9), which allows the selection of stable transfectans in mammalian cells with the antibiotic G418. Cloned DNA is expressed as a fusion protein with EGFP, which allows a fluorescent detection of the native protein in living cells.

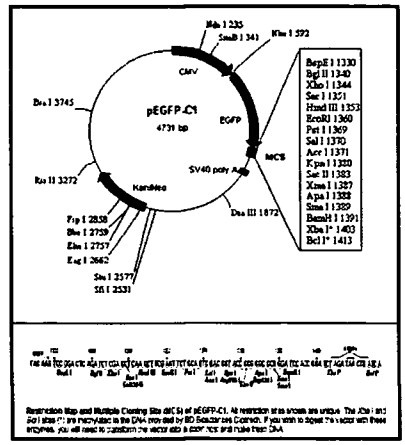

Fig. 9: Circular vector map of pEGFP-C1 and its MCS (clontech cataloque)

4.1.3 pEGFP-C3-WRN

The pEGFP-C3 vector, a variant of the pEGFP-C1 vector, contains an SV40 promotor, neomycin/kanamycin resistance and poly A signals from thymidine kinase as well. WRNs coding sequence has been cloned into this vector by M. Denegri, allowing a transient overexpression of WRN-EGFP fusion protein.

4.1.4 E1A

The Adenoviral Minigene E1a has been cloned into a pCMVSV vector, containing the cytomegalovirus (CMV) promoter/enhancer and the simian virus (SV) 40 polyadenylylation region. The pCMVE1a was generated by insertion of the pSP4-E1a into the pCMVSV vector (Yang, Bani, Lu, Rowan, Ben-David, et al. 1994), kindly provided by M. Denegri.

4.1.5 Exo70

Exo 70 is an essential 70 kDa subunit of the exocyst complex of *S. cerevisia.* As a whole, the exocyst complex fuses protein carrying vesicles to the plasma membrane, in order to enable cytosis (TerBush, Maurice, Roth, and Novick 1996). Full length Exo70, the coiled-coiled (CC) region and delta CC (Full length Exo70 without CC-region) have been cloned into PCI neo vectors (the vectors were kindly provided by M. Löscher, K.Lee).

4.1.6 WRN and SNEV

SiRNAs targeting WRN and SNEV were purchased from Dharmacon. 5 nmol of lyophilised siRNA were diluted in 250 µl of siRNA Buffer (Dharmacon 5x Buffer diluted in nuclease free and sterile water) and 10 µl aliqotes with a concentration of 20 pmol/µl were immediately frozen and stored at -80°C. The siRNA should not be thawn and frozen again.

4.2 Generation of SNEV deletion mutants

The primers were designed in a way that SNEV full length (the whole coding sequence of SNEV nucleotides 1-504), SNEV delta 67 (68-504; lacking the U-box), SNEV delta 91 (92-504), SNEV delta 206 (207-504, WD40 region), SNEV 206 (1-206; lacking the WD40 region) inserts could be obtained (Fig. 10 A). $SNEV^{Prp19/Pso4}$ and parts of $SNEV^{Prp19/Pso4}$ should be ligated into two vectors: PCI-neo and pEGFP-C1.

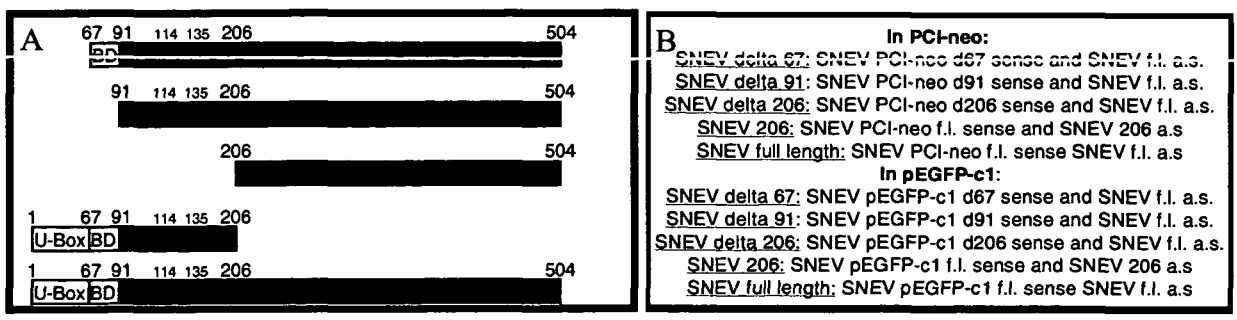

Fig. 10: (A) Functional structure of the SNEV Inserts; delta 67, delta 9, delta 206, 206, full length (B) Primers used for the synthesis of the SNEV Inserts

Additional to the SNEV coding sequence binding sites the primers also contain restriction sites for EcorI (sense primers) and XhoI (antisense primers). For the cloning of PCI-neo plasmids his tags were added to the sense primers. Since the two plasmids contain the same restriction sites in their MCS the same antisense primers could be used for both plasmids

4.2.1 Polymerase chain reaction (PCR)

PCR is a quick and easy method for the amplification of small amounts of DNA. The reaction is running in three steps repeated for several times. In the first step the reaction mixture is heated up to 94°C, which leads to denaturation of the template DNA and the primers. In the next step the reaction is cooled down to the annealing temperature of the primer, depending on the GC/AT ratio and the length of the primer, allowing the primer to anneal to the complementary single stranded sequence of the template. In the third step thermophile polymerase is synthesising new DNA strands starting from one primer and producing double stranded DNA (Fig. 11).

Reagents	
Sense primer	1 µl (10 pmol)
Antisense primer	1 µl (10 pmol)
Template	1 µl (10-50 ng/µl)
dNTPs	0,5 µl (10 mM)
Gotaq buffer	10 µl (5x)
DNA GoTaq Polymerase	0,5 µl (200U/µl)
AD	36 µl

Tab. 1 Composition of the PCR reaction mixture

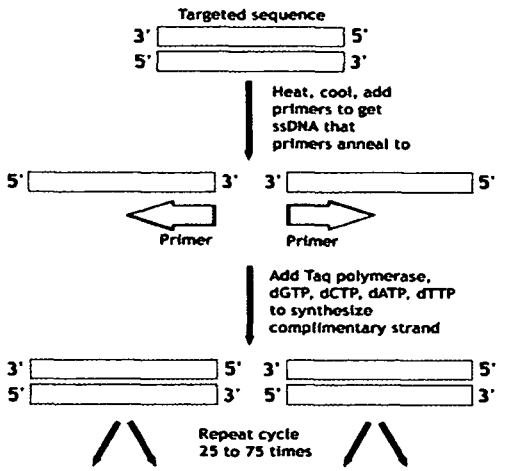

Fig. 11: Steps of a poly chain reaction (PCR)

The PCR reaction mixture was set up as described in Tab. 1. A vector, containing SNEV was used as a template and the corresponding primers were chosen according to Fig.10 (B). The PCR was run for 20 cycles, minimizing the risk of mutation.

4.2.2 DNA purification after PCR

The Wizard SV Gel and PCR Clean up system from Promega is used for the purification of DNA after PCR, reverse transcription and gel electrophoresis. The DNA is binding to a silica column in the presence of high concentrations of chaotropic salts, which leads to a precipitation of the DNA by deprivation of water molecules. The impurities are removed by several washing steps using ethanol.

The PCR product or the DNA Gel band was added to the same amount of membrane binding solution and centrifuged for 1minute at full speed. The flowthrough was discarded and two washing steps with ethanol were performed, each step followed by centrifugation. After the ethanol was completely evaporated the DNA was eluted with 50 µl nuclease free water (NFW).

4.2.3 Quantification of DNA

4.2.3.1 Agarose gel electrophoresis

Electrophoresis is used to separate molecules based on their size. For the separation of DNA fragments an agarose gel electrophoresis is the method of choice. DNA, which possesses negative charges, migrates in an electric field towards the anode. Larger DNA molecules are thereby moving slower than smaller ones. ethidiumbromide is used for the visualisation of DNA under UV. The amount and the molecular mass of the DNA can be estimated using a DNA marker.

The DNA samples were mixed together with a 6x loading dye (Fermentas) and brought on a 1% TAE agarose gel. For quantitative analysis the electrophoresis was carried out at 120 V, for qualitative analysis at 90 V in TAE buffer containing ethidiumbromide.

4.2.3.2 Photometer

The concentration of nucleic acids can also be determined by measuring the optical density (OD) at 260 nm (nucleic acids) and 280 nm (protein). The ratio of $OD_{260/280}$ should be above 1,80 implicating that the solution is pure and without contaminants.

4.2.3.3 Bioanalyzer®

DNA quantity and quality can be measured with a DNA lab chip from Agilent Technologies in the Agilent 2100 Bioanalyzer®, a capillary electrophoresis system, following the same operation procedure as for the quantification of RNA, but using a DNA chip and a DNA ladder mix. (see. Quantification of RNA; Bioanalyzer®)

4.2.4 Restriction

Restriction enzymes are enzymes originally isolated from bacteria that are able to recognize specific short DNA sequences and cut the DNA at these specific sites, thereby providing a defence mechanism to viral infection. Today also artificial restriction enzymes, recognising nearly every DNA sequence, are available. In order to be able to ligate designated DNA into an expression vector, the vector and the insert have to be cut with the same restriction enzymes, so that they are ligated together, forming a plasmid with the desired properties.
The pCI-neo and the pEGFP-C1 Vector as well as the inserts were digested with two restriction enzymes, namely EcoRI and XhoI. The digestion was performed at 37°C, the usual working temperature of most enzymes, in EcoRI buffer and 1% BSA for 2-3 hours. The enzymes, the buffer and the BSA were purchased from NEB (New England Biolabs). After the incubation the enzymes were deactivated by heat. The restriction fragments were purified by qualitative gel electrophoresis and Promega® Wizard SV Gel and PCR Clean up system.

4.2.5 Ligation

To join the cohesive ends that remain after the digestion with restriction enzymes DNA ligase is used. The ATP dependent ligase is able to religate the molecules together, by enabling the 3' OH group to covalently bind to the 5' phosphate group again.
T4 ligase (NEB), T4 ligase 10 x buffer (NEB) containing ATP and the digested vector and insert were mixed together and incubated at 22°C for ½ - 1 hour. The molar vector/insert ratio should range from 1:5 to 1:10. Thereafter ligase was inactivated by heat (70°C 5 min). The plasmid was precipitated by adding 96% ethanol (2,5 x volume of the ligating reaction solution) and sodiumacetate (0,1 x volume of the ligating reaction solution) followed by an incubation at -20°C for about ½ hour. After centrifugation (at -4°C for 10 minutes at full speed) the DNA precipitate was washed with 70% ethanol and centrifuged for another 10 minutes. After the complete removal and evaporation of the ethanol the DNA was dissolved in 10 µl NFW.

4.2.6 Electroporation

The electroporation is a mechanical transformation method, which allows polar molecules to surpass the membrane barrier. A quick voltage shock may disrupt the membrane temporarily, allowing polar molecules to get into the cell.
Electrocompetent *E.Coli* (DH10B) were grown in LB medium at 37°C, while shaking, until the culture reached an optical density of 0,6 - 0,8 at 600 nm. The bacteria were harvested and washed extensively with 1mM HEPES buffer. Then the pellet was resuspended in 10% glycerin, aliquotet, frozen with liquid nitrogen and stored at -80°C. The ligated and ethanol precipated plasmid and the electrocompetent *E.coli* aliquot is mixed together, put into an electroporation cuvette and a short electric pulse of 2.5 kVolt, 1000 Ohm and 25 µFarad was applied. After a short regeneration period in a full medium (S.O.C.) the bacteria were plated on an antibiotic containing selection medium and incubated at 37°C for 24 hours.

4.2.7 PCR screening of positive clones

Colonies that had grown on the selective medium were verified to contain the vector/insert plasmid and not only the empty vector by PCR. The PCR was performed by using primers that were flanking the restriction sites of the vectors in order to generate the MCS alone (negative clone) or the MCS with the desired insert (positive clone). The positive and negative clones were distinguished by their length on an agarose gel. Positive clones were amplified, the plasmid purified with a Miniprep purification Kit and sequenced.

4.2.8 Purification of DNA with a Miniprep purification Kit (Promega)

For purification of DNA a Miniprep purification Kit from Promega was used, following the instructions. 1 - 10 ml of antibiotic containing medium were inoculated with a single colony and incubated over night. The bacteria were harvested by centrifugation and completely resuspended in 250 µl of cell resuspension solution. 250 µl of cell lysis solution were added and mixed. After adding 10 µl of alkaline protease solution the solution was incubated for 5 minutes at room temperature. 350 µl of neutralization solution was added, centrifuged, the supernatant was applied on a column and centrifuged again. After two washing steps with ethanol containing washing solution and the total evaporating of the ethanol the DNA was eluted with 100 µl of NFW (nuclease free water).

4.2.9 Sequencing

Sequence analysis is mostly performed with the Sanger method. In this method, synthetic nucleotides, lacking the OH group at the 3'carbon (didesoxynucleotides), therefore not able to bind another nucleotide, are integrated in a linear amplification reaction. During the elongation of the DNA strand the incorporation of such ddNTP leads to a stop; the method therefore is also called the chain termination method. The reaction requires a template, a primer, DNA polymerase and a mixture of normal dNTPs and ddNTPs. Each different ddNTP

(ddATP, ddGTP...) is labelled with another fluorescing colour. Thus the incorporation of a ddNTP results in an elongation stop, many different lengths of DNA strands appear, each with one labelled ddNTP at the end. The different fragments are separated by length and the sequence determined by scanning the fluorescing ddNTPs.
The sequencing was performed by Martin IBL.

4.2.10 Endofree maxiprep

Endotoxins, also known as lipopolysaccharides (LPS) are membrane components of gram-negative bacteria. Endotoxins are released during the lysis of bacteria in plasmid purification and can significantly reduce transfection efficiency in cell lines.
A single colony of the plasmid, containing the desired insert was picked and 100 ml of selective medium (medium with antibiotics) were inoculated and incubated over night at 37°C and vigorously shaking. The bacteria were lysed under alkaline conditions (P2) and cleared on a QIAfilter Maxi Cartridge. The endotoxin removal buffer (ER) was added to the filtered lysate and the cleared lysate was loaded onto the anionexchange tip where plasmid DNA selectively binds under appropriate low-salt and pH conditions. RNA, proteins, metabolites, and other low-molecular-weight impurities were removed by a medium-salt wash (QC) and ultrapure plasmid DNA was eluted in high-salt buffer (QN). The DNA was concentrated and desalted by isopropanol precipitation and ethanol wash.

4.3 Cell culture

4.3.1 Cell lines

4.3.1.1 HeLa

HeLa, an epithelial like cervix carcinoma cell line, was established by George O. Grey in 1952. HeLa cells were named after their donator, a woman named Henrietta Lacks.
HeLa cells were cultivated in RPMI 1640 basal medium, supplemented with 4mM L-glutamine and 10% FCS (fetal calf serum, Hyclon). HeLa cells were grown adherent in roux flasks till reaching confluency. Confluency and possible contaminations were periodically monitored by microscopy and mycoplasmen tests. The cells were subcultered twice a week. Therefore, the supernatant was removed, the cell layer was washed once with PBS and trypsinized with 0,5 ml trypsin (0,1% trypsin, 0,02% EDTA)/T25 roux flask. After detachment, trypsin action was inhibited by adding culture medium containing FCS and the cell suspension was split at a ratio of 1:20 for continuous culture. The cells were always incubated at 37°C and 5% CO_2.

4.3.1.2 U2-OS

The U2-OS cell line, originally known as the 2T line, was isolated from the bone tissue of a fifteen-year-old girl suffering from osteosarcoma. It was established in 1964 and exhibits epithelial adherent morphology. U2-OS stably overexpressing either vector containing siRNA targeting WRN or scrambled siRNA (Eller, Liao, Liu, Hanna, Backvall, et al. 2006) were kindly provided by V.A. Bohr.
The two cell lines were named U2-OS/WRN KD and U2-OS control. Both U2-OS cell lines were cultivated in DMEM (Dulbecco's Modified Eagle's Medium) basal medium, supplemented by 4 mM L-glutamine, 200 µg/ml hygromycin B and 10% FCS. Degree of confluency and possible contaminations were monitored by microscopy and mycoplasmen

tests. For passaging, the supernatant was removed and then the cell layer was washed twice with PBS. Thereafter, 0,5 ml trypsin solution (0,25% trypsin, 0,02% EDTA)/T 25 roux flask were added and the flask was incubated at 37°C until detachment. The U2-OS WRN/KD cells detached easier when compared to the U2-OS controls, but were quite sensitive to typsinisation. After detachment trypsin action was inhibited by adding culture medium containing FCS and the cell suspension was split at a ratio of 1:6 to 1:8. The cells were always incubated at 37°C and 5% CO_2.

4.3.2 Mycoplasma test

Mycolasma are very small bacteria lacking a peptidoglycan cell wall. Their cell membrane contains cholesterol compounds, similar to eucaryotes. Therefore, mycoplasma are resistant to antibiotics targeting the cell membrane, like penicillin. Mycoplasma infection is hard to recognize, because it is not immediately killing the cell and is not detectable under the microscope, like other microbial infections. Thus, periodical mycoplasma tests are essential in cell culture.

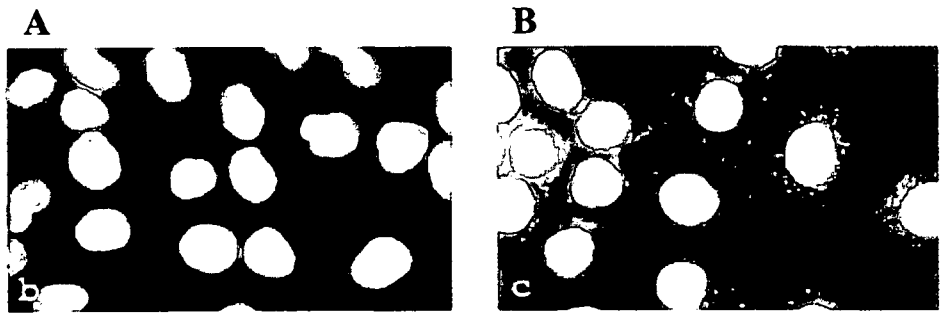

Fig. 12: Mycoplasm uninfected (A) and infected (B) HeLa cells stained with DAPI (Nir-Paz, Prevost, Nicolas, Blanchard, and Wroblewski 2002)

For detecting a mycoplasma infection the cells were stained with the DNA binding dye 4',6-Diamidino-2-phenylindol (DAPI), that fluoresce under UV. In healthy cells only the clear nuclei can be seen. Infected cells show hazy fluorescence outside of the cell's nuclei, representing DNA of mycoplasma as seen in Fig. 12. Cells, seeded into 8-chamberslides, were incubated over night at 37°C. The medium was removed, the cell layer was washed with PBS and incubated with cold DAPI staining solution (1 µg DAPI/ml methanol) for 10

minutes. The slides were air dried and samples were analysed using a fluorescence microscope.

4.3.3 Calculation of cell number

For the determination of the cell number the cells were counted with a counting chamber from Bürker–Türk. The counting chamber contains a deeping of 0,1 mm^3 (~ 0,1 µl) when sealed with a cover glass. On the engraved net 9 squares can be seen (Fig. 13). The cells were harvested and 500 µl of the cell suspension was mixed with 100 µl of Trypan Blue. The cell suspension was transferred to the counting chamber and the number of living and dead cells was counted. The number of viable cells and the viability of the cell suspension were determined using following equations:

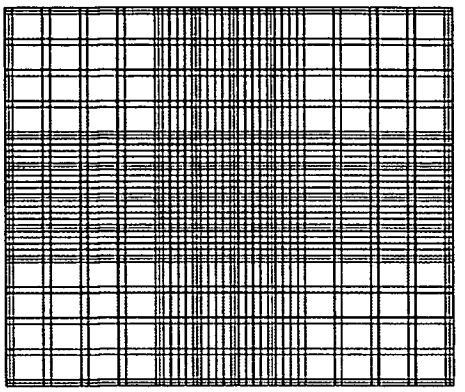

Fig. 13 A Bürker -Türk counting chamber, showing the counting net [www.zaehlkammer.de]

$$viable\ cells/ml = \frac{counted\ viable cells}{number\ of\ counted\ squares} x\ 12000$$

$$dead\ cells/ml = \frac{counted\ dead\ cells}{number\ of\ counted\ squares} x\ 12000 \qquad \%\ viability = \frac{viable cells}{total\ cell\ number} x100$$

4.3.4 Calculation of population doublings

The population doubling level (PDL) reveals the age of a cell line. In other words it tells you how many times these cells have divided. The PDL is a function of cumulative population doublings calculated following this equation:

$$PD = \frac{\log\left(N/No\right)}{\log 2}$$

N = number of cells No = number of cells plated

To establish a growth curve the PDL was plotted against the days of cultivation.

4.3.5 Cryopreservation

4.3.5.1 Freezing of cells

The cells were grown to 90% confluency in T 75 roux flasks, sufficient for 3 cryopreservation vials. The cells were trypsinised, diluted in approximately 9 ml of FCS containing medium and centrifuged. The pellet was resuspended in 3 ml chilled freezing medium, aliquoted in crypreservation vials and frozen at -80°C for 24 - 48 hours, before being transferred to liquid nitrogen.

4.3.5.2 Thawing of cells

After the cell suspension had thawn, the cells were immediately pipetted into precooled culture medium and centrifuged. Since the DMSO (Dimethylsulfoxid) in the freezing medium is toxic for the cells this step had to be performed very quickly. The pellet was resuspended in culture medium, transferred into a T 25 roux flask and incubated at 37°C. The cells were microscopically monitored and when the cells had reached confluency (after 24 - 48 hours), they were passaged.

4.3.6 Transfection

4.3.6.1 Lipofection

Cationic lipid-vesicles are binding anionic DNA, fusing with the cell membrane and thereby transferring the plasmid into the cell. HeLa cells were transfected at a confluency of 70 - 90% for DNA and 30 - 50% for siRNA transfections, using a defined amount (Tab. 2) of

Lipofectamine™ 2000 (LA2000, Invitrogen) according to the manufactures instructions. Therefore, LA2000 was diluted in Opti-MEM® I Reduced Serum Medium (Invitrogen) and incubated for 5 minutes. In between the appropriate amount of plasmid DNA or RNA was diluted in Opti-MEM® according to Tab. 2 as well and the two solutions were combined, mixed gently and incubated for 20 minutes. The cell culture medium was removed and exchanged with Opti-MEM®. The lipid-DNA/RNA complex was added to the cells and after an incubation of 4-6 hours a medium change was performed.

Plasmid DNA				
Culture vessel	Vol. of plating medium	Vol. of dilution medium	DNA	LA 2000
12-well	1 ml	2 x 100 µl	1,6 µg	4 µl
6-well	2 ml	2 x 250 µl	4 µg	10 µl
T25 (roux flask)	5 ml	2 x 500 µl	8 µg	20 µl
iRNA				
Culture vessel	Vol. of plating medium	Vol. of dilution medium	siRNA	LA 2000
12-well	1 ml	2 x 100 µl	40 pmol	2 µl
6-well	2 ml	2 x 250 µl	100 pmol	5 µl
T25 (roux flask)	5 ml	2 x 500 µl	200 pmol	10 µl

Tab. 2: Amounts of Optimem, LA2000, and DNA/RNA used for lipofection

When transfecting DNA, GFP was introduced as a positive control and a transfection without DNA was used as a negative control. For transfections of siRNAs, control siRNAs were introduced as a negative control.

For cotransfection of DNA and siRNA cells were seeded into 6-well plates to reach 50% confluency at time of transfection. Whereas, the same amounts of RNA and DNA were used as for the transfection of RNA or DNA alone (Tab. 2) the amount of LA2000 was doubled.

For the transfection of two plasmid DNAs, cells were grown in T 25 roux flasks to 80 - 90% confluency. Thereafter, 2 µg of E1a plasmid, 4 µg of Exo 70 variants [Exo70 full length, Exo70 delta CC and Exo70 CC] plasmid and 20 µl of LA2000 were used for transfection.

In order to down regulate two proteins simultaneously, a cotransfection with two siRNAs was performed. 6 well plates were treated with 50pmol of each siRNA instead of the normally recommended 100 pmol (Tab. 3).

	SNEV	SNEV/ WRN	WRN	Control
SNEV siRNA	50 pmol	50 pmol	-	-
WRN siRNA	-	50 pmol	50 pmol	-
Control siRNA	50 pmol	-	50 pmol	100 pmol

Tab. 3: siRNA cotransfection of WRN and SNEV, SNEV and WRN alone and the control

4.3.6.2 Nucleofection

Nucleofection is a new and fast electroporation-based transfection method that enables the DNA to enter the nucleus directly.

Due to the low transfection efficiency of lipofection with the U2-OS cells, nucleofection was the method of choice. Therefore, $1*10^6$ cells were centrifuged, the pellet was resuspended in 100 µl cell line nucleofection solution Kit V (freshly prepared) and combined with 2 µg of plasmid DNA. The solution was transferred into an AMAXA cuvette and electroporated using the programme X-01. Thereafter, the cell solution was transferred into a 6-well plate, containing 2 ml of prewarmed culture medium and incubated at 37°.

4.4 Protein analysis

4.4.1 Cell and protein isolation

Cells were detached and centrifuged for 10 min at 170 rpm. The pellet was resuspended in PBS, centrifuged and washed again with PBS. The supernatant was properly removed and the cell pellet was resuspended in 50 µl of NEB (Nuclear Extraction Buffer) thus breaking up membranes and setting free proteins. The solution was centrifuged twice through a

QIAshredder (QIAgen) for 2 minutes at full speed, to shear DNA which could interfere with the following analysis. The protein lysate was shock frozen in liquid nitrogen and stored at -80°C until further use.

4.4.2 Determination of protein concentration (Bradford)

The Bradford assay is one of the most common protein quantification methods. Under acidic conditions, the Bradford dye is most stable in its doubly-protonated red form. When binding to aromatic amino acids in proteins, however, the unprotonated blue form becomes more stable. The absorbance can be measured at 595 nm. The Bradford dye assay was carried out in 96-well plates, able to measure 8 samples simultaneously (Fig. 14).

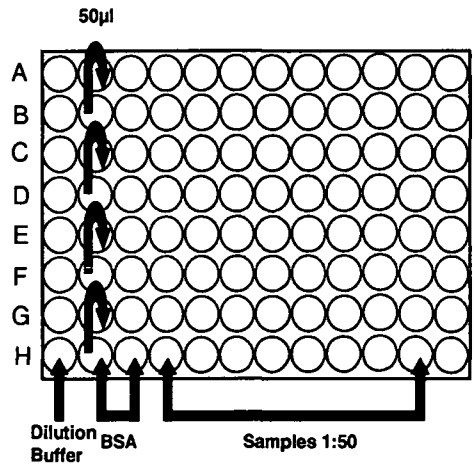

Fig. 14: Dilution steps for Bradford assay in a 96 well microtiter plate

100 µl of the 1:50 diluted samples, the blank (dilution buffer alone) and the standard solution (200 µg/ml BSA) were pipetted into the first row (H1-H11). In the remaining rows (G-A) 50 µl of dilution buffer was added. 1:2 dilutions were performed, using a multichannel pipette (50 µl from row H → G, G→ F; etc...). After diluting the Bradford dye (BioRad) 1:5, 150 µl were added to each well, the plate was incubated for 5 minutes on a shaker and detected with a Photometer (ELISA reader). The data were evaluated with the Magellan software.

4.4.3 SDS-PAGE

SDS PAGE (Sodiumdodecylsulfate Polyacrylamid Gelelectrophorese) involves the separation of proteins based on their size. By heating the sample in a buffer containing reducing (Mercaptoethanol) and denaturing (SDS) reagents, proteins become unfolded and coated with SDS detergent molecules, thereby getting a high negative charge. When loaded onto a gel matrix, which is placed in an electric field, the negatively charged proteins migrate towards the anode and are separated by their molecular weight. The proteins can be detected by a non specific visualization method, like silver stain or by antibody specific detections e.g. western blotting. The molecular mass can be estimated by compairing with standards of known molecular weight.

For the protein separation NuPAGE® Bis-Tris gels (4 - 12%) from Invitrogen were used. After estimation of protein concentration by Bradford assay, 20-30 µg of protein were mixed with 2x SDS-loading dye and denaturated by boiling for 10 minutes. The samples and a protein standard were applied to the gel, fixed in the XCell *SureLock*™ Mini Cell gel caster. The XCell *SureLock*™ was filled with NuPAGE® MOPS SDS-running buffer and an electric field of 200 Volt was applied. The gel ran for about 1 hour till the marker band had reached the bottom of the gel. The gel was removed from the cover and further used for western blot or silverstaining.

4.4.4 Silverstaining

Silverstaining is a method, which allows the visualization of proteins after SDS PAGE, by the binding of silver ions to aminogroups. The gel was first treated with a fixation buffer for 1 hour or over night. The gel was then incubated for 15 minutes with incubation buffer, washed with AD (de-iomized water) and incubated in $AgNO_3$ solution for 10 minutes. The development was performed until the bands had reached the desired intensity and the reaction was stopped by adding stop solution. The gel was stored at 4°C in 10% glycerine.

4.4.5 Western Blot

Western blot analysis can detect one protein in a mixture of proteins and gives you information about the size of the protein. After separating the protein mixture on a matrix gel normally done by SDS PAGE, the proteins are blotted on a membrane in an electric field which drives the negatively charged proteins out of the gel into the membrane. Single proteins can then be detected by incubating the membrane with a primary antibody, which binds specifically to the protein of interest. A second antibody, recognising the first antibody is enzyme labelled. After incubation in a specific enzyme solution, the protein can be detected.

After SDS PAGE the gel was laid on a PVDF membrane surrounded by transfer buffer soaked spoons. This "sandwich" was put into the XCell *SureLock*™ Mini Cell gel casting chamber, the blotting module was closed and a current of 30 V and 170 mA for 90 minutes was applied. Then the membrane was blocked in a 3% skim milk TPBS Buffer for 1 hour at room temperature or over night at 4°C. The primary antibody solutions were prepared according to Tab. 4 and the blot was incubated in this solution for 1 hour while shaking. The blot was washed 3 times for 10 minutes with TPBS and then the secondary antibody, labelled with peroxidase, was applied (Tab. 4) followed by further incubation for 1 hour.

Primary Antibody		
Mouse anti-SNEV PRP19 688	1:2.500 in TPBS	
Rabbit anti WRN	1:1.000 in TPBS 3% skimmed milk	
Rabbit anti β-Actin	1:5000 in TPBS 3% skimmed milk	
Secondary Antibody		
Anti-mouse IgG	1:10.000 in TPBS 3% skimmed milk	PO-conjugated
Anti-rabbit IgG	1:10.000 in TPBS 3% skimmed milk	PO-conjugated

Tab. 4: Reaction solutions of primary and secondary antibodies used in western blotting

After washing the membrane 3 times for 10 minutes, the blot was incubated with a freshly prepared peroxidase reaction solution for 5 minutes and the chemiluminescence was detected on a Typhoon 9400 Imager. For quantification the membrane was stained for the housekeeping gene β-actin as well.

4.5 RNA analysis

4.5.1 RNA isolation

4.5.1.1 Trizol® RNA isolation

Trizol® (Invitrogen), a monophasic solution of phenol and guanidine, is used for RNA isolation. Trizol® maintains the integrity of the RNA while disrupting the cell membrane and dissolving cell components. After adding chloroform, three phases appear: the protein containing phenol-chloroform phase, the intermediate phase (precipitated DNA) and the RNA containing aqueous phase.

About $5*10^6$ cells (~T 25 Roux flask) were collected and washed twice with PBS. The cell pellet was thoroughly resuspended in 1ml Trizol® and stored at –80°C in sarstedt tubes until use or 200 µl of chloroform were applied immediately and mixed well by vortexing for 15 seconds. After 2 - 4 minutes incubation at room temperature the phases were separated by centrifugation (4°C, 12.000 g, 15 min). The aqueous phase, containing the RNA, was carefully removed and transferred into a fresh Sarstedt tube. 500 µl of isopropanol was added and the suspension was mixed gently by converting the tube several times. After 10 minutes incubation at room temperature, the RNA was precipitated by centrifugation (4°C, 12.000 g, 10 min). The supernatant was removed and the pellet was washed by adding 500 µl 70% ethanol following another centrifugation step (4°C, 7.500 g, 5 min). The ethanol was carefully removed by pipetting and the RNA pellet was air-dried thereafter, the RNA was resuspended in NFW water at a heating block (60°C for 10 minutes.). The RNA solution was stored at -80°C until further use.

4.5.1.2 RNA isolation with the RNeasy Mini Kit

The RNeasy kit (Qiagen) provides a high-salt buffer system allowing up to 100 µg of RNA longer than 200 bases to bind to the RNeasy silica membrane.

Cells cultured in 6 well plates were first lysed in the presence of a highly denaturing guanidine-thiocyanate containing buffer (350 µl RLT), which inactivated RNases followed by homogenization by centrifugation using QIAEshredder tubes. 350µl Ethanol was added to provide appropriate binding conditions, and the sample was then applied to an RNeasy Mini spin column, where the total RNA bound to the membrane. In order to digest residual DNA, 80 µl of freshly prepared DNAse solution was applied on the column and incubated for 15 minutes. Thereafter, contaminants were efficiently washed away (2 x 350 µl RW1, 2 x5 00 µl RPE). The RNA was resuspended in RNase free water and stored at -80°C. The amount of RNA was measured by UV-absorption and RNA Biolanalyzer® assay, which could additionally predict the RNA quality. The RNA was further used for reverse transcription and Real time PCR.

4.5.2 RNA quantification

4.5.2.1 Bioanalyzer®

The Agilent 2100 Bioanalyzer® is a capillary electrophoresis system, which is integrated in a chip, able to measure 12 samples simultaneously. A standard marker normalises the retention time and a standard ladder mix is used to quantify and qualify the samples (Fig. 15). For the measurement of RNA samples a nano RNA Agilent lab chip was used. The measurement was performed according to the manufactures instruction. Briefly, the gel dye mix was freshly prepared and 9 µl were pipetted on the chip. The priming station was closed and the plunger pressed for 30 seconds. Another 9 µl were added to each well. After heating up the samples and the RNA ladder to 75°C, avoiding secondary structure, 1µl of the samples or the ladder mix were pipetted in each of the 12 sample wells and the well for the ladder. The chip was shaken heavily, followed by the analysis in the 21000 Bioanalyzer®, using the total mRNA program.

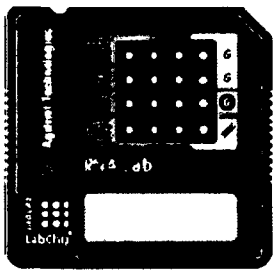

Fig. 15: Nano RNA Agilent lab chip

4.5.2.2 Agarose Gel

Electrophoresis is used to separate molecules based on their size. For the separation of nucleotides an agarose gel electrophoresis is the method of choice. Charged molecules move within an electric field and molecules get thereby separated by the difference of their size. A denaturing gel system, using formaldehyd, is more recommendable in order to avoid extensive secondary structures of RNA molecules. Ethidiumbromide is used for the visualisation of RNA under UV. The amount and the molecular mass of the RNA can be estimated using a RNA marker.

About 2 µg of RNA sample were mixed together with a 2 x RNA loading dye (Ambion) and the samples were denaturated at 65°C for 10 minutes. Agarose was melted in DEPC water and MOPS buffer and formaldehyde were added. The gel was casted into the gel chamber and after polymerisation the samples were loaded on the gel. An electric current of 65 mA was applied for about 2,5 hours.

4.5.3 Reverse transcription

The reverse transcriptase is an enzyme naturally occurring in reverse-transcribing viruses. These viruses need the reverse transcriptase to transcribe their RNA genome into DNA, which then can be integrated into the host genome where it can be replicated.

For our reverse transkription we used M-MLV, reverse transcriptase from the *Moloney murine leukemia virus*. Trizol® or RNeasy Kit isolated RNA was quantified (see RNA Quantification) and 1 µg of total RNA was mixed with 1 µl oligo dT_{18} (500 ng/µl) and incubated for 5 minutes at 70°C. Reverse transcriptase reaction mix (Tab.5) was added and the reverse transcription reaction was performed at 55°C for 1 hour, followed by a purification of the cDNA in order to get rid of non transcribed RNA and components of the reaction mix. Therefore 2 µl NaOH (2,5 M) were added to the cDNA solution and incubated for 10 minutes at 37°C, whereby residual RNA got denaturised. After the neutralisation with HEPES the cDNA was purified by using a *Wizard SV Gel and PCR Clean up system* from Promega. The cDNA was stored at -20°C until further use.

Reagents	
dNTPs	0,5 µl (10 mM)
first strand buffer 5x	4 µl
DTT	1 µl (0,1 M)
Superscript II RNase H- (reverse transcriptase)	1 µl (200 U/µl)
RNAse OUT (RNAse inhibitor)	
AD and RNA/oligodT18	1 µl (40 U/µl)
Total Volume	20µl

Tab. 5: Composition of the reverse transcription reaction mix

4.5.4 Real time PCR

Real-time polymerase chain reaction (qRT-PCR) allows the quantification of certain genes in "real time", measuring the DNA increase during amplification. The quantification is performed by fluorescent dyes (e.g SYBR green) binding to total dsDNA. The amplification follows a curve, which at the beginning, until detectable amounts are present, is very flat followed by an exponential phase ending in a plateau, at the limit of saturation. The more primed cDNA (and thus mRNA) is present, the earlier it will be detected during the cycles of amplification. Comparing template curves with standards of exactly known concentration the amount of the cDNA of a specific gene can be measured exactly. To get to know the total copy numbers of a gene a reference control, a house keeping gene, has to be measured as well.

Two qRT-PCRs were set up for our analysis, one run measuring a housekeeping gene (GAPDH) giving information about the integrity and the concentration of the cDNA samples, and one measuring the target gene (WRN, SNEV). The standard for the detection of WRN gene had to be generated by PCR with designed real time primers specific for WRN. Two primer pairs were tested. PCR was performed in 45 cycles and the melting temperature was varied from 55°C – 65°C but no product could be detected. A second PCR, using the product of the first PCR as template was set up as well and generated detectable amounts of product.

Standards of SNEV and GAPDH already existed. For each run standard curves with known copy numbers had to be established. 19 µl of the PCR mix (Tab. 6) were transferred into PCR tubes and 1 µl of the dilutions of the standard curve or the template was added. Each of the samples was measured in triplicates, the standard dilutions in duplicates.

Reagents	
SYBR Green Super Mix 2x	10 µl
Sense primer	1 µl (10 pmol)
Antisense primer	1 µl (10 pmol)
Template/standard	1 µl
NFW	7 µl
Total Volume	20 µl

Tab. 6 Composition of the Real time PCR mix

The qRT-PCR was performed using a Rotor Gene 2000 Real time Cycler (Corbett Research) with a 36 well carousel rotor. The Rotor Gene 2000 Real time Cycler was run for 45 cycles, starting with a denaturising step at 95°C (15 sec), following an annealing step at 55°C (5 sec) and ending with two extension steps at 72°C (15 sec) and 80°C (20 sec). An additional melting curve was acquired, by rising the temperature 1°C each second in a temperature range of 65 - 99°C, to control the correct amplification of the target sequence.

4.6 Analysis of stress response

4.6.1 Reagents

4.6.1.1 H_2O_2 (Hydrogen peroxide)

H_2O_2 is a clear liquid with strong oxidizing properties and is a powerful agent for generating ROS and therefore oxidative stress. 0,88 M (3%) H_2O_2 (Sigma) was diluted in cultivation medium, prior to use.

Testing concentration dependency: U2-OS/WRN-KD and U2-OS control cells were treated with different concentrations (5 - 100 mM) of H_2O_2 for 2,5 hours, the medium was changed and after a regeneration period of 21,5 hours apoptosis and necrosis was measured (see 4.6.2).

Testing time dependency: 300 µM H_2O_2 was added to the cells and apoptosis/necrosis was measured after 10, 20, 40, 60, and 120 minutes.

Treatment in suspension: Cells were collected and resuspended in H_2O_2 containing medium (0,3; 0,5 and 1 mM). After 2 hours the percentages of apoptosit and necrotic cells were measured.

4.6.1.2 BSO/Bleomycin

Bleomycin induces single strand DNA breaks, probably by inhibiting the incorporation of thymidine and is used as a drug in cancer treatment. BSO creates ROS and therefore oxidative stress and DNA damage.

Stock Solution: 50 mg of BSO (Sigma) were dissolved in 1 ml AD, sterile filtered and stored at 4°C. 10 mg of bleomycin (15 U, Sigma) were dissolved in 5 ml sterile physiological saline solution and aliquots were stored at -20°C. Stock solutions were diluted in culture medium to reach the final concentrations.

U2-OS/WRN-KD and U2-OS control cells were cultivated in medium, containing 1 mM of BSO, for 24 hours. Thereafter, medium was changed and media containing different concentrations (50 - 200 µM) of bleomycin were added. After 48 hours of incubation at 37°C apoptosis/necrosis was measured.

4.6.1.3 Cisplatin (cis-diamminedichloroplatinum(II)

Cisplatin acts by crosslinking DNA in several different ways, making it impossible for rapidly dividing cells to duplicate their DNA for mitosis. Therefore, Cisplatin is used as anti-cancer drug (chemostatic) with quite a bunch of side effects.

Stock Solution: 10 mg of Cisplatin (kindly provided by the Institute of Inorganic Chemistry, Vienna) were suspended in 500 µl DMSO, aliquoted and stored at -20°C, protected from light. An appropriate amount of stock solution was directly diluted in culture medium to reach the final concentrations.

U2-OS/WRN-KD and U2-OS control cells were incubated at 37°C in Cisplatin containing medium for 24 hours and apoptosis/necrosis was measured. The siRNA treated HeLa cells were incubated for 9,5 hours in Cisplatin containing medium at 37°C and thereafter apoptosis/necrosis was measured.

4.6.1.4 KP1019 (indazolium trans-[tetrachlorobis(1H-indazole)ruthenate (III))

K1019 is a new ligation developed at the Institute of Inorganic Chemistry, Vienna. It gets into the cell by binding to transferrin or albumin using the transferrin receptor. KP1019 has been shown to be quite successful in the treatment of solid tumours, which show altered physiological conditions, involving the over-expression of transferrin receptors due to a higher iron demand.

Stock solution: 28,5 mg of KP1019 (kindly provided by M Jakupec, Institute of Inorganic Chemistry, Vienna) were suspended in 1ml of DMSO and stored at room temperature. Stock solution was further diluted in culture medium to the desired final concentrations.

U2-OS/WRN-KD and U2-OS control cells were incubated with medium containing KP1019 (50-100 μM) for 24 hours and the cells were counted thereafter. The decrease of cell number and therefore the rate of necrosis was calculated.

4.6.2 Apoptosis assay /Annexin V/PI

In contrast to necrosis, which is a form of cell death resulting from acute cellular injury, apoptosis is carried out in an orderly process. Apoptosis, also called programmed cell death, is a process involving biochemical and morphological cellular changes such as loss of membrane asymmetry and attachment, condensation of the cytoplasma and nucleus and internucleosomal cleavage of DNA. Once triggered it cannot be stopped. Series of biochemical cascades are taking place and the cell is following the "apoptotic programme" until cell death. Apoptosis can be triggered by DNA damages or viral infections, preventing cancer formation or the spread of an infection to other organs.

One of the early morphological changes of apoptosis is the loss of membrane integrity, leading to the exposition of PS (Phosphotidylserine), normally part of the inner membrane layer (Fig.16 A). Annexin V FLUOS (Roche) is binding to PS in the presence of Ca^{2+} and due to the labelling with FITC (fluoresceinisothiocyanate) it can be detected by flow cytometry. Since necrotic as well as apoptotic cells bind PS, cells were additionally stained with PI (propidium iodide), a DNA binding dye, which is only able to reach the nucleus when

disrupted membranes are present. Since only necrotic and late apoptotic cells stain for PI we could easily discriminate viable cells from early apoptotic and necrotic cells/late apoptotic cells (Fig.16 B).

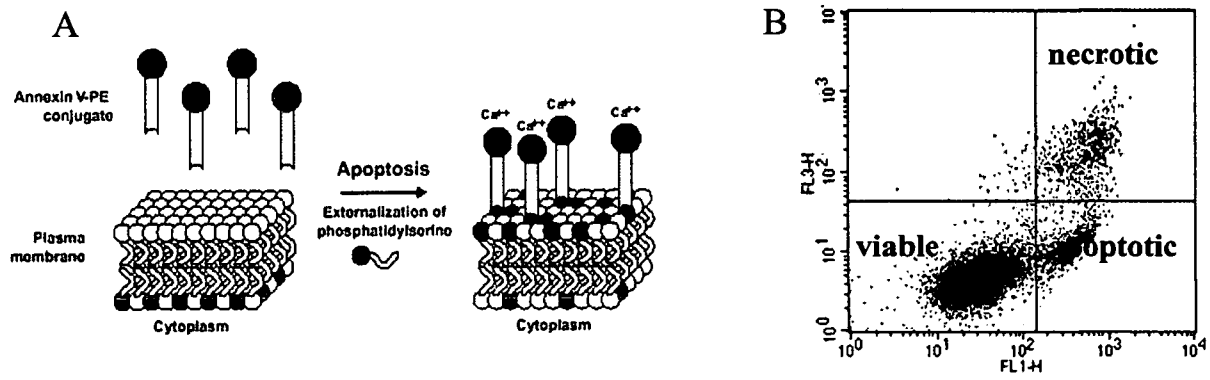

Fig.16: (A) Alteration of cell membrane during apoptosis, exposing PS, which is binding to AnnexinV in the presenve of Ca^{2+} [www.bdbioscience.com]; (B) Measurement of apoptotic and necrotic cells by FACS; lower left no PI and FITC staining (living cells), lower right FITC but no PI staining (early apoptotic cells), upper right PI and FITC staining (necrotic cells, late apoptotic cells)

For determination of the percentages apoptotic/necrotic cells the cell layer was washed twice with PBS and trypsinized. Thereafter, the cells were resuspended in PBS supplemented with Mg^{2+} and Ca^{2+} and 10% FCS. The cell suspension was centrifuged at 170 g for 10 minutes and the pellet was once washed with Annexin V binding buffer. After centrifugation the pellet was suspended in 50 µl of Annexin V-FITC/PI reaction Buffer, incubated for 10 minutes and analyzed using flow cytometry (FACSCalibur, BD).
For compensation controls were measured as well (cells stained with PI or Annexin V alone). The analysis was performed using an excitation wavelength of 488 nm and a 515 nm filter for the detection of FITC (Fl-1) and filte above 600 for PI detection (Fl-3).

The viability of U2-OS cells treated with H_2O_2 was calculated by subtraction of percentages of apoptotic and necrotic cells, determined by apoptosis analysis. For cells treated with Cisplatin the increase in apoptotic and necrotic cells, referring to control cells was calculated.

4.6.3 Splicing assay using E1a

E1a is an adenoviral Minigene. By transfecting cells with this Minigene, three important alternative splicing products are generated (13s, 12s and 9s splicing variants) (Fig. 18). Shifting of the ratio of the spliced mRNA products can occur by alternative splicing.

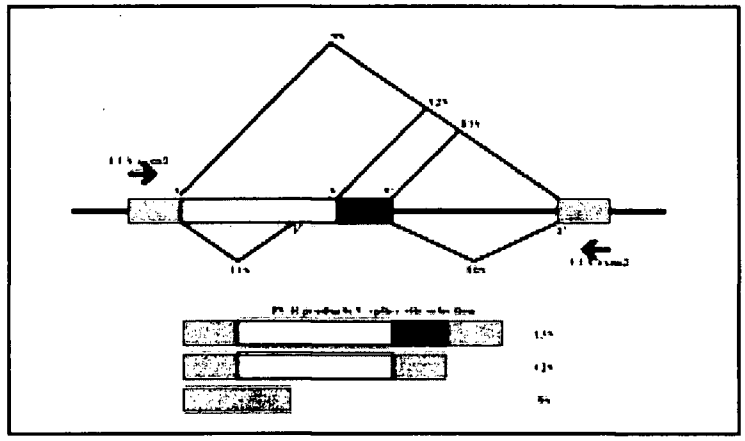

Fig. 18: Mechanism of alternative splicing of E1a

4.6.3.1 Exo 70

Getting to know the process of the E1a splicing assay, HeLa cells were co-transfected with the Exo70 plasmids (Exo70 full length, Exo70 delta CC and Exo70 CC) and E1a. After 24 hours the RNA was isolated and the mRNA was reverse transcribed. After the PCR, E1a splicing variants were quantified with Bioanalyzer®.

4.6.3.2 WRN

U2-OS WRN-KD and U2-OS control cells were transfected with the adenoviral Minigene E1a using nucleofection. After 24 hours incubation the total RNA was isolated using the RNeasy Kit, reverse transcribed and the splicing products were quantified by addition of radioactive [32P] dCTPs to the PCR, which was performed at the University of Dundee, Scotland by M. Denegri.

Furthermore HeLa cells were transfected with E1a and pEGFP-C3-WRN plasmid, transiently overexpressing WRN. The transfection, mRNA isolation, reverse transcription and the splicing assay was performed by M. Denegri at the University of Dundee, Scotland.

5 Results

5.1 Construction of SNEV deletion mutants

Although the PCRs for insert preparation were run with a low number of cycles and new primers were synthesized the plasmids showed a high number of mutations. The cloning procedures weren't successful. Only one construct could be cloned: The pEGFP-C1 vector containing SNEV coding sequence, lacking the first 67 aminoacids the U-Box (delta 67 SNEV pEGFP-C1). In order to determine the transfection efficiency HeLa cells were transfected with the purified, endofree delta 67 SNEV pEGFP-C1 plasmid using lipofection the expression of EGFP was monitored after 24 hours by flow cytometry (Fig. 19 A). The efficiency of the transfection was measured by comparison of the EGFP-fluorescence with the fluorescence of untreated HeLa cells. A transfection efficiency of about 50% was calculated (Fig.19 B).

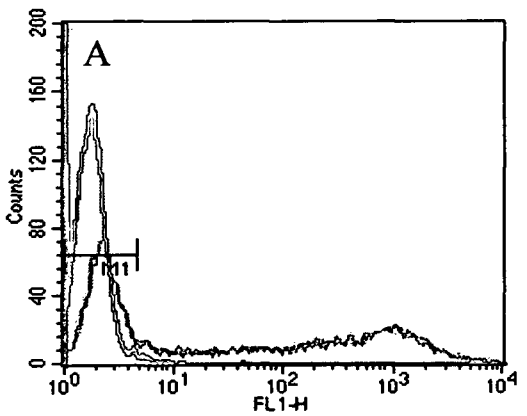

B

	Percentage negative (M1)	Percentage positive
HeLa control	99,19	0,89
EGFP	51,03	48,97

Fig. 19: (A) Measurement of fluorescence by flow cytometry; Untreated HeLa cells (red), pEGFP expressing cells (green); (B) Percentages of counted cells within the marker M (negative cells)

5.2 Characterisation of U2-OS

In order to get to know more about the effects a WRN deprivation had on cells, the stable U2-OS WRN/KD cell line was compared with U2-OS control cell. The morphology, the growth characteristics and the expression of WRN and SNEV$^{Prp19/Pso4}$ was analyzed.

5.2.1 Morphology

The U2-OS cells show the typical epithelial cell morphology. The cells are flat and growing to dense cell layers. As demonstrated in Fig. 20 the two cell lines show no morphological differences.

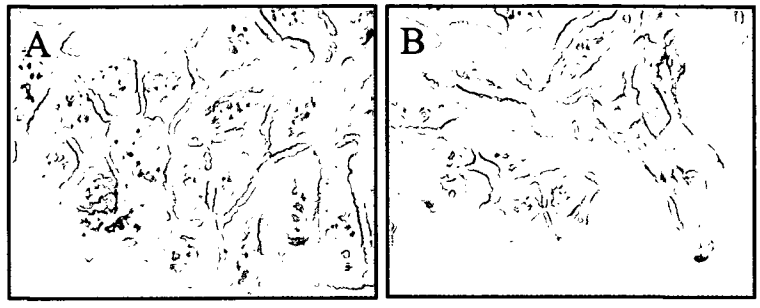

Fig. 20: (A) U2-OS WRN/KD cells, (B) U2-OS control cells, both showing the typical epithelial cell morphology. No morphological differences are obvious.

5.2.2 Cultivation properties

The U2-OS cell lines were quite hard to detach, therefore the cell layer had to be washed twice and the prewarmed trypsin was used in a higher concentration (0,25%). Since U2-OS WRN/KD cells were additionally quite sensitive to the trypsinisation, it was necessary to monitor the detachment, leaving the trypsin only as long as absolutely necessary on the cells. In general the U2-OS cells were quite robust and could be passaged with high splitting ratios, without losing their excellent growth properties.

5.2.3 Growth characteristics

Although cells isolated from WS patients had been described to have reduced growth potential, the stable WRN depleted cells showed no such obvious differences in growth characteristics, when compared to the U2-OS control cells.

Both cell lines were growing at he same growth rate and as seen in Fig. 21 during the 100 days of cultivation no differences were visible.

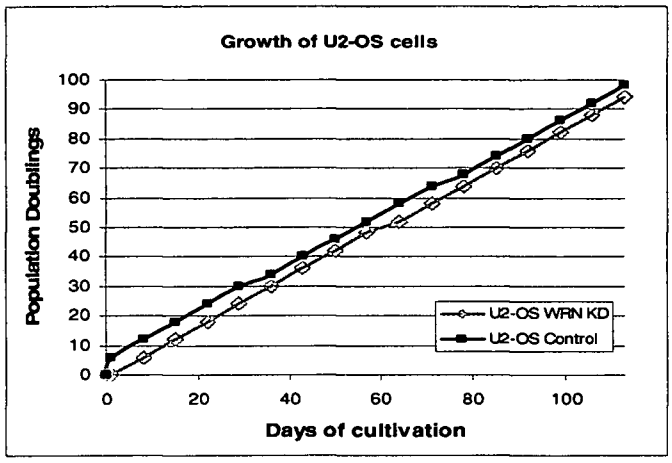

Fig: 21: Growth curves of U2-OS control and U2-OS WRN/KD cells

5.2.4 Expression level of WRN and SNEV$^{Prp19/Pso4}$

In order to confirm the decrease in expression of WRN in the knock down cell line a westernblot analysis, using an antibody targeting WRN, was performed. As shown in Fig. 22 (A) the U2-OS WRN/KD cells didn't express the WRN protein anymore. In contrast U2-OS control cells did express WRN protein with a clear band at about ~180 kDa. The native protein has a molecular weight of 167 kDa, strongly suggesting that the detected band represents the WRN protein. As WRN and SNEV$^{Prp19/Pso4}$ had been shown to physically interact in processing DNA repair, WRN KD could also affect the expression level of SNEV$^{Prp19/Pso4}$. Therefore a westernblot analysis targeting SNEV was carried out as well. In Fig. 22 (B) a clear band for SNEV at 55 kDa can be seen. For quantification of the protein bands the expression of β-actin, a housekeeping gene, was

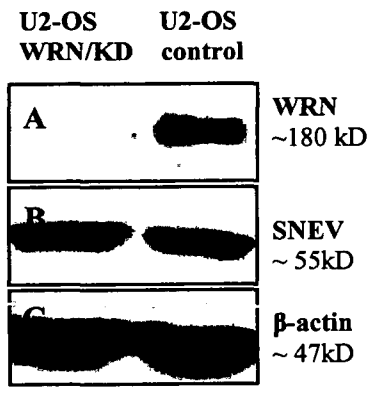

Fig. 22: 30 µg of protein lysate of U2-OS WRN7KD (1.lane) and U2-OS control (2.lane) protein were loaded on a gel and detected for WRN (**A**) SNEV$^{Prp19/Pso4}$ (**B**) and β-actin (**C**) by westernblot

measured as well (Fig. 22 C). However no difference between U2-OS WRN/KD and U2-OS control cells is obvious. In this set up the down regulation of WRN doesn't affect the expression of $SNEV^{Prp19/Pso4}$.

5.3 Stress response

5.3.1 U2-OS cell line

5.3.1.1 H_2O_2

In order to get to know how WRN depleted cells react on oxidative stress U2-OS WRN/KD and U2-OS control cells were treated with H_2O_2. Fig. 23 shows U2-OS cells, treated with 500 µM H_2O_2 for 2 hours. In both cell lines many dead cells could be seen. However, no differences between the two cell lines were visible.

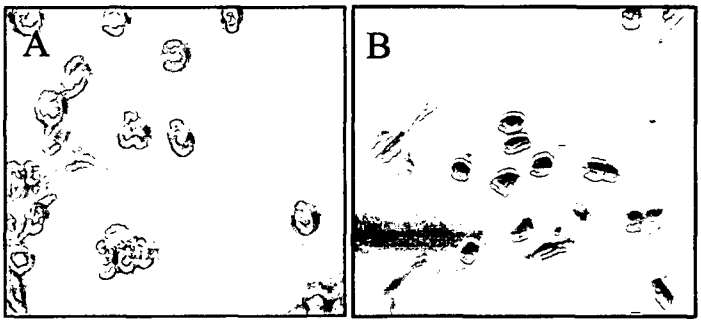

Fig. 23 (A) U2-OS WRN/KD cells and (B) U2-OS control cells after 2 hours of incubation with 500 µM H_2O_2

Fig. 24 (A) shows the percentages of living cells in U2-OS WRN/KD and U2-OS control cell lines after treatment with different concentrations of H_2O_2. It seems that U2-OS WRN/KD cells reacted more sensitive to the treatment with H_2O_2 but the starting viability was very low. In Fig. 24 (B) the percentages of living cells after different incubation periods with 300 µM

can be seen. In this set up the WRN depleted cells seemed to be more robust to the treatment with H_2O_2. Since these two experiments gave no clear hint about differences in the sensitivity of U2-OS WRN /KD cells and U2-OS control cells they were treated in suspension, as well. As shown in Fig. 24 (C) both U2-OS cell lines showed no significant effect on the treatment with H_2O_2. The viabilities of both cell lines were higher than 90% independent of the amount of applied H_2O_2.

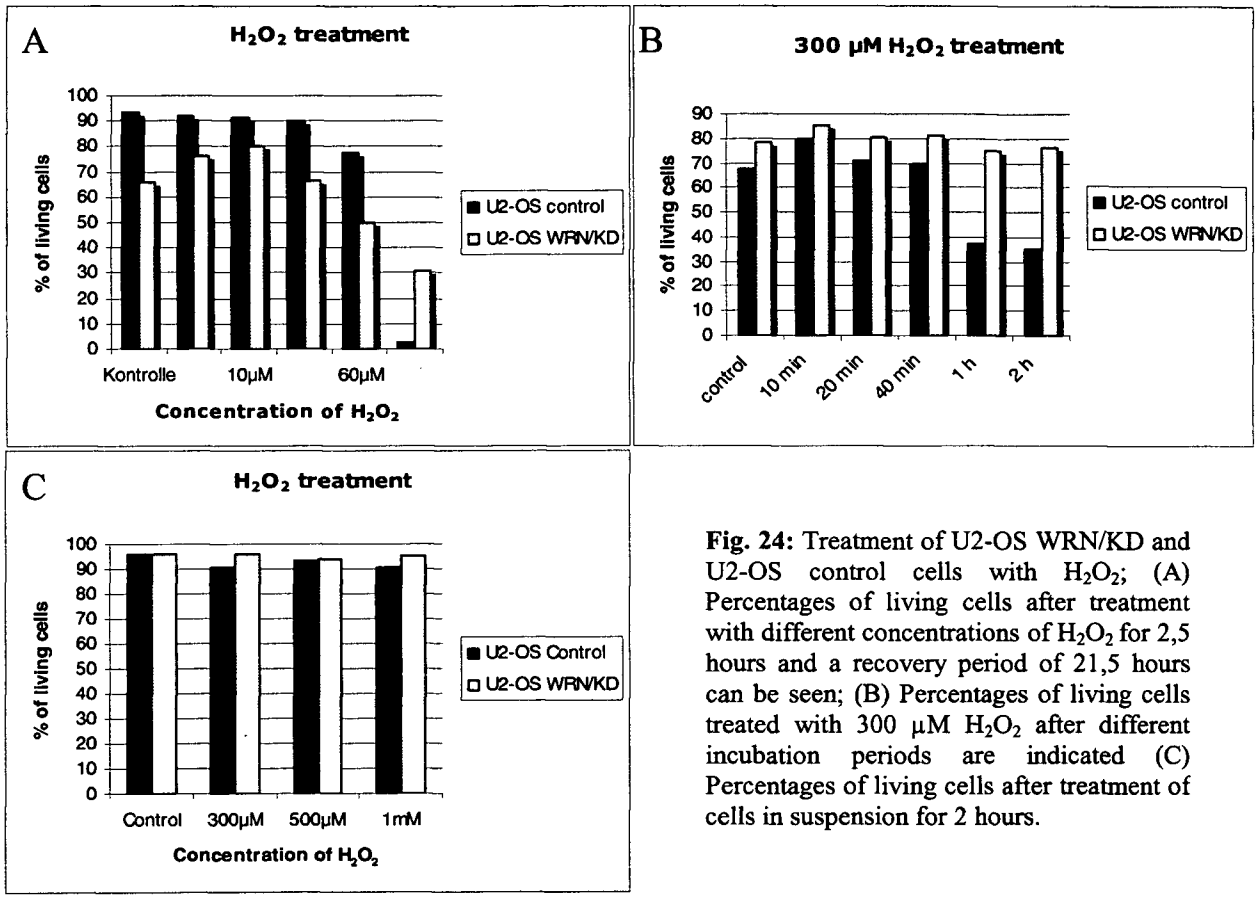

Fig. 24: Treatment of U2-OS WRN/KD and U2-OS control cells with H_2O_2; (A) Percentages of living cells after treatment with different concentrations of H_2O_2 for 2,5 hours and a recovery period of 21,5 hours can be seen; (B) Percentages of living cells treated with 300 µM H_2O_2 after different incubation periods are indicated (C) Percentages of living cells after treatment of cells in suspension for 2 hours.

Since all assays were performed differently it is difficult to compare these experiments. No conclusions about differences between the two cell lines in aspect of coping with H_2O_2 related DNA damage can be drawn.

5.3.1.2 KP1019

U2-OS WRN/KD and U2-OS control cells were treated with 50-100 µM KP1019 for 24 hours. After the incubation the cells looked bursted (Fig. 25), much cell debris could be seen but no apoptotic or dead cells. Since the cell debris can't be measured by apoptotic assay, the cells were counted and the decrease of cell number was calculated. In Fig. 26 the decrease in living cells of U2-OS WRN/KD and U2-OS control cells can bee seen.

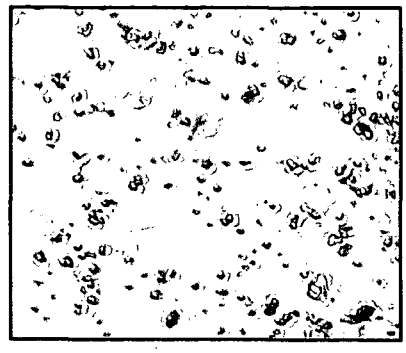

Fig.25: U2-OS cells treated with 100µm KP1019, adherent and bursted cells can be seen

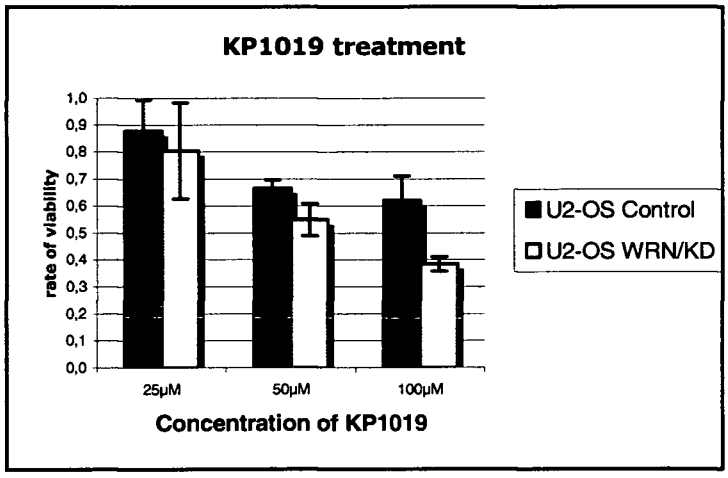

Fig. 26: Decrease in living cells of U2-OS WRN/KD and U2-OS control cells after 24 hours KP1019 treatment. Error bars indicate the standard aberration of three independent experiments

After a treatment with 100 µM KP1019 the WRN/KD cells show about 20% lower viability rate than control cells. Control cells seem to be more resistant to KP1019 treatment than the WRN depleted cells, suggesting WRN playing a role in the protection or damage repair of KP1019 induced lesions.

5.3.1.3 Cisplatin

Cisplatin, a platin ligation is a drug, used in tumour therapy. Cisplatin is able to inhibit the replication of rapidly dividing cells by its ability to crosslink DNA. These ICL lesions can be repaired through the HR and NER repair mechanism, which WRN has been found to play a

role in. U2-OS WRN/KD and U2-OS control cells were treated with Cisplatin. Fig. 27 shows representative microscopic pictures of the U2-OS WRN /KD and U2-OS control cells treated with 100 µM Cisplatin. After 24 hours more apoptotic and necrotic cells can be seen in the WRN depleted cells.

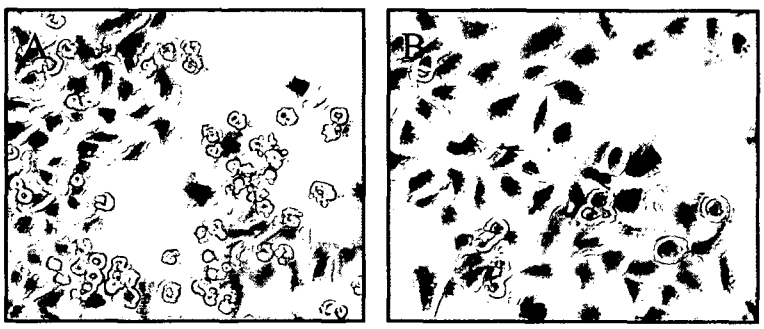

Fig. 27: (A) U2-OS WRN/KD cells and (B) U2-OS control cells treated with 100µM cisplatin for 24 hours

In Fig. 28 the increase of apoptotic and necrotic U2-OS WRN/KD cells after a 24 hours treatment with Cisplatin in comparison to the U2-OS controls can be seen. Whereas treatment with 200 µM Cisplatin increased the percentages of apoptotic and necrotic cells beyong 80% in U2-OS WRN/KD cells, only about 55% of U2-OS control cells died.

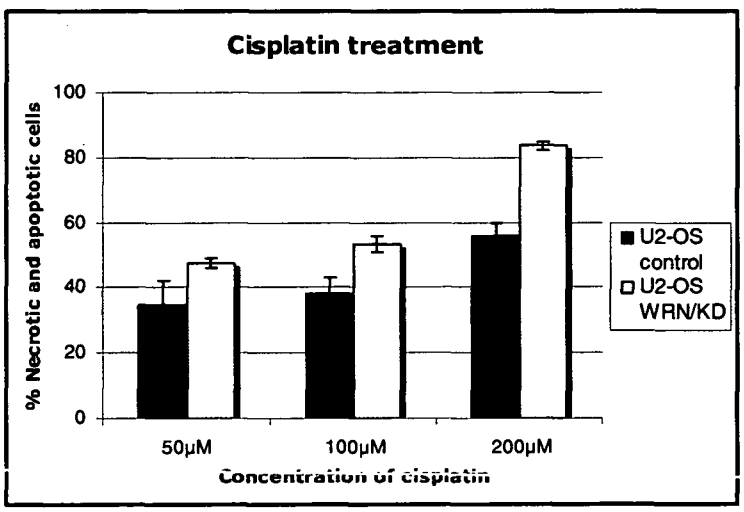

Fig.28: Percentage of apoptotic/necrotic U2-OS WRN/KD and U2-OS control cells after 24 hours Cisplatin treatment. Error bars indicate the standard aberration of three independent experiments.

These data confirm the suggested role of WRN in the repair of ICLs.

5.3.2 Knock down of WRN and SNEV$^{Prp19/Pso4}$

In order to get to know more about the interaction between WRN and SNEV$^{Prp19/Pso4}$ a simultaneous down regulation of both proteins using siRNA was aimed. The WRN and SNEV$^{Prp19/Pso4}$ depleted cells were treated with Cisplatin, in order to monitor their ability to cope with this DNA damaging substance. Cells depleted of WRN and SNEV$^{Prp19/Pso4}$ alone were taken as controls.

5.3.2.1 Downregulation SNEV$^{Prp19/Pso4}$

HeLa cells were transfected with different concentrations of SNEV$^{Prp19/Pso4}$ siRNA and after 24 hours the cells were harvested and the protein expression as well as the downregulation on mRNA level was analyzed

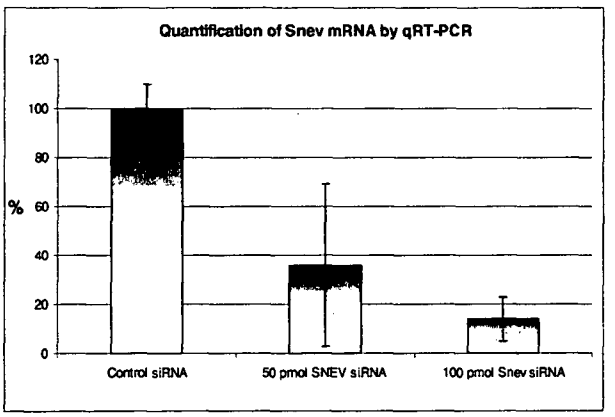

Fig. 29: qRT-PCR detecting SNEV$^{Prp19/Pso4}$ mRNA after SNEV siRNA treatment. Error bars indicate standard aberrations of three independent experiments

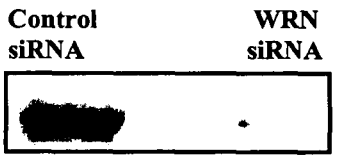

Fig.30: Western blot, detecting SNEV$^{Prp19/Pso4}$ 24 hours after treatment with 100 pmol control and SNEV siRNA

In Fig. 30 the decrease of SNEV$^{Prp19/Pso4}$ protein expression after siRNA treatment can be seen. The data of real time PCR confirm a significantly downregulation of SNEV$^{Prp19/Pso4}$ on mRNA level (Fig. 29).

5.3.2.2 Downregulation WRN

In order to confirm the ability of the siRNA to specifically target WRN protein, the down regulation was monitored by westernblot. In Fig. 31 a decrease of protein expression can be seen. The siRNA is therefore able to significantly down regulate the expression of WRN after 24 hours.

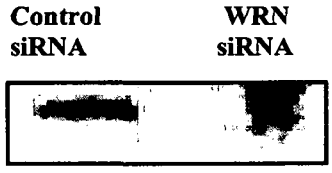

Fig.31: Westernblot, detecting WRN 24 hours after treatment with 100 pmol control and WRN siRNA

5.3.2.3 Downregulation of WRN and SNEV$^{Prp19/Pso4}$

The simultaneous downregulation of the two proteins WRN and SNEV$^{Prp19/Pso4}$ was important in order to get to know something about the interaction of these proteins while exposed to genotoxic stress. In order to deplete the cells of WRN and SNEV$^{Prp19/Pso4}$, the cells were treated with two siRNAs targeting WRN and SNEV$^{Prp19/Pso4}$ at the same time. In Fig. 32 decrease of WRN protein can be seen in the WRN and WRN/ SNEV$^{Prp19/Pso4}$ siRNA treated cells, whereas in the control and the SNEV$^{Prp19/Pso4}$ siRNA treated cells WRN can be clearly detected.

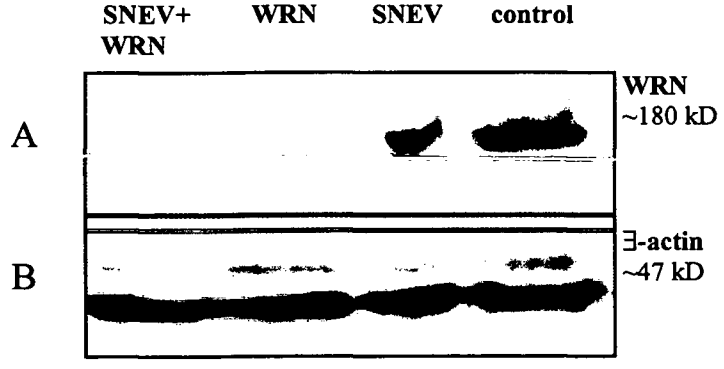

Fig. 32: Westernblot detecting (A) WRN and (B) β-actin of SNEV$^{Prp19/Pso4}$ and WRN siRNA treated cells as well as HeLa cells treated with WRN siRNA, SNEV$^{Prp19/Pso4}$ siRNA and control siRNA alone

5.3.2.4 Cisplatin treatment

In this experiment we tried to find out which effects the lack of both proteins can have, while being exposed to Cisplatin. HeLa cells were transfected with siRNAs targeting WRN and $SNEV^{Prp19/Pso4}$, WRN and $SNEV^{Prp19/Pso4}$ alone and a non-targeting control siRNA and treated with Cisplatin for 9 hours. Thereafter the percentages of apoptotic and necrotic cells were determined. In Fig. 33 the increase in necrotic and apoptotic cells after treatment with 200µM Cisplatin can be seen.

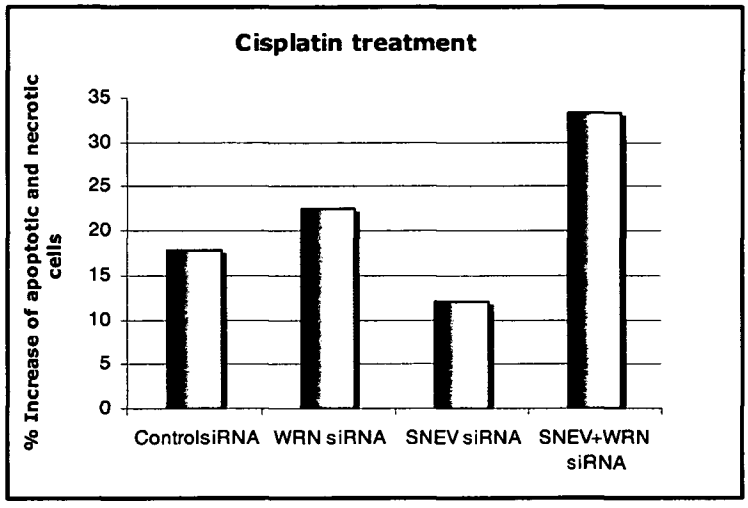

Fig. 33: Increase in apoptotic and necrotic cells after treatment with 200 µM Cisplatin for 9 hours

The simultaneous WRN/$SNEV^{Prp19/Pso4}$ downregulation of HeLa cells shows the greatest increase in dead cells. The cells lacking these two important proteins seem to be more sensitive to the applied stress when compared to cells lacking WRN or $SNEV^{Prp19/Pso4}$ alone.

5.4 Splicing

5.4.1 Set up experiment

In this assay a possible role of Exo70, a part of the exocyst complex, in splicing should be determined. In Fig. 34 the E1a splicing variants of the three Exo 70 transfectans (Exo70 full length, Exo70 delta, CC and Exo70 CC,) and the controls (pCI-neo, pEGFP) can be seen.

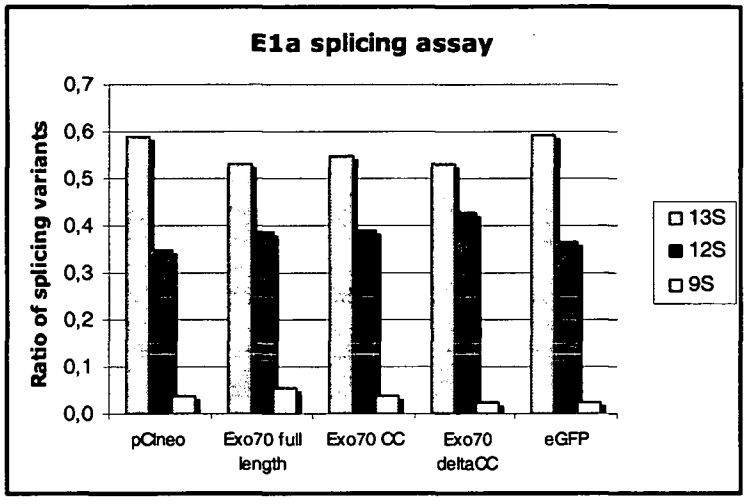

Fig. 34: Ratio of splicing products 13s, 12s, 9s of Exo70 full length, Exo70 delta CC and Exo70 CC and the controls pCI-neo and pEGFP

The three Exo70 variants are only showing slight differences in their splicing pattern. The PCI-neo splicing control and the pGFP control get equally spliced. Due to these results no conclusion about the involvement of Exo70 in the splicing process can be predicted.

5.4.2 WRN and splicing

5.4.2.1 Splicing assay in U2-OS WRN KD and U2-OS control

For getting more insights into WRN's hypothesized role as a possible splicing factor, a splicing assay was set up. Therefore, the RNA of U2-OS WRN/KD and U2-OS control cells, transfected with the adenoviral Minigene E1a, was isolated and reverse transcribed. The E1a splicing variants were quantified using a PCR with a radioactive labelled dCTPs (performed by in Dundee, Scotland by M. Denegri). Fig. 35 shows the molar ratio of the splicing variants. The U2-OS WRN/KD cells show an about ten time fold increase of the 9s variant at the expense of the 13s splicing type.

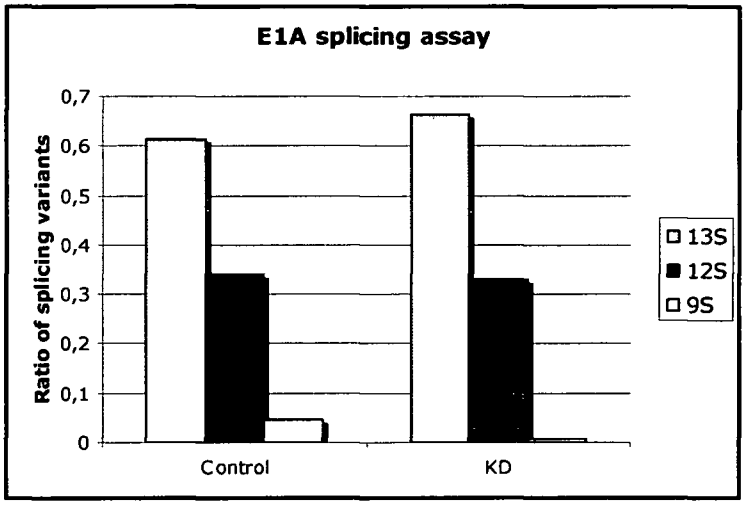

Fig. 35: WRN: Ratio of splicing products (13s, 12s, 9) in U2-OS WRN/KD and control cells transfected with E1a

This analysis suggests a potential role of WRN in alternative splicing. However, further experiments have to be performed in order to verify the observed result.

5.4.2.2 Splicing in transiently WRN overexpressing cell line

Getting more insights in the hypothesized role of WRN in splicing an splicing assay with transiently WRN overexpressing cells was performed as well. In order to determine whether the cells are expressing the fusion protein a FACS analysis was performed and a transfection

efficiency of 30% was measured (data not shown). Additionally a westernblot detecting WRN/EGFP fusion protein was carried out as well. In the westernblot (Fig.36) detecting WRN two bands can be seen. Endogenous WRN and an additional band with a molecular mass of about 250 kDa, detecting WRN-GFP fusion protein can be seen. The two bands can't be distinguished that well, due to low resolution in the range of high molecular mass. To get information about WRN's splicing properties a splicing assay was performed with HeLa cells transfected with different concentrations of pEGFP-C3-WRN and E1a plasmid (generated by M. Denegri).

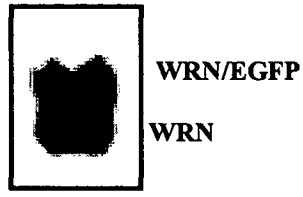

Fig. 36: Westernblot detecting WRN in WRN-pEGFP-C3 fusion protein expressing HeLa cells

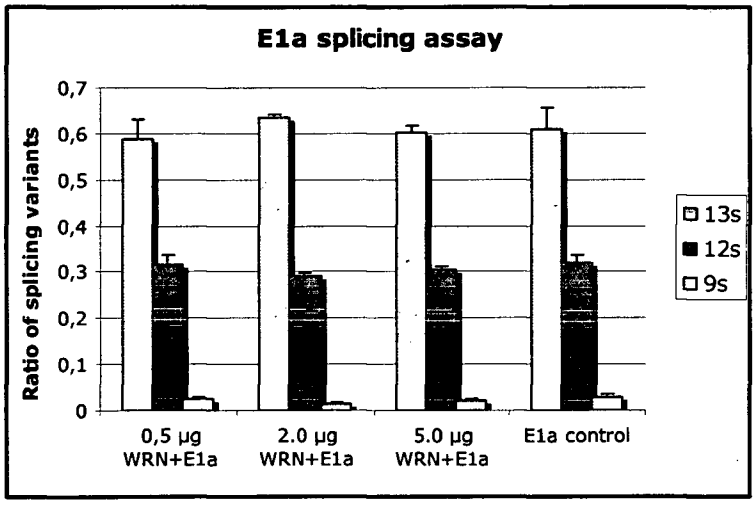

Fig.36: Ratio of splicing products (13s, 12s, 9) of transiently WRN overexpressing HeLa cells, transfected with different concentrations of pEGFP-C3-WRN with standard aberrations of the triplets

As demonstrated inFig.36 no apparent differences between the WRN overexpressing and the HeLa cells transfected with E1a alone are visible.

6 Discussion and conclusion

6.1 Characterisation of WRN/KD cells

WRN depleted U2-OS cells, kindly provided by V.Bohr, were compared to their control U2-OS cell line, still possessing WRN activity. Morphology and growth were observed. Surprisingly, no differences in growth could be seen, although cells isolated from WS patients exhibit genomic instability, replication defects, aberrant telomere maintenance and decreased proliferation potential in vitro. This phenomenon could be explained by the fact that U2-OS, as a tumour cell line exhibits severe chromosome abnormalities. Tumour cells have already escaped a natural proliferation stop since mechanisms responsible for cell cycle control are inactivated. The p53, a key cellular component in maintaining genomic stability (Haupt, Berger, Goldberg, and Haupt 2003), (Hofseth, Hussain, and Harris 2004) is for example mutated in many tumour cell lines. WRN has been found to bind to p53 in *vivo* and WS patient's derived fibroblasts show attenuated ability to undergo p53-mediated apoptosis (Spillare, Robles, Wang, Shen, Yu, et al. 1999). The negative effects on growth, evoked by the absence of WRN, could be irrelevant when p53 is already displaying altered properties. However, the same observed growth capacities of WRN/KD and the control cell line do not disapprove nor approve WRN's proposed role in replication and growth. These observations have been made in a tumour cell line and therefore could not be unconditionally adopted as a universally valid fact.

6.2 Stress response of WRN/KD cells

As mentioned above WRN has been proven to play an important role in many different DNA damage repair processes (Cheng, Kusumoto, Opresko, Sui, Huang, et al. 2006; Cooper, Machwe, Orren, Brosh, Ramsden, et al. 2000; Eller, Liao, Liu, Hanna, Backvall, et al. 2006;

Harrigan JA 2006; Otterlei, Bruheim, Ahn, Bussen, Karmakar, et al. 2006). In order to confirm these data cells were treated with different toxic reagents evoking oxidative stress, genotoxic stress or both. The first reagent which we tried out was H_2O_2, a strong oxidizing reagent, which we have already proven to evoke a concentration depent effect on HeLa cells (data not shown). We tried out many different experimental set ups, but were not able to find concentration dependent induction of necrosis or apoptosis in U2-OS. The data we generated showed strong variations. Therefore, we started to test other stress inducing reagents. U2-OS cells were treated with BSO folowed by incubation with Bleomycin. Although this protocol worked fine with HUVECs overexpressing $SNEV^{Prp19/Pso4}$ (Voglauer, Chang, Dampier, Wieser, Baumann, et al. 2006) these two toxic reagent showed no effect on U2-OS cells. Finally, we found Cisplatin and KP1019 that are described to be able to evoke cell death and apotosis (Fuertesa, Castillab, Alonsoa, and Perez 2003; Kapitza, Jakupec, Uhl, Keppler, and Marian 2005). Cisplatin possesses chemotherapeutic properties by crosslinking DNA in several ways, making it impossible for rapidly diving cells, such as tumour cells, to undergo mitosis anymore. After 24 hour Cisplatin treatment a dose dependent effect on induction of necrosis/apoptosis was seen. WRN/KD cells showed a 30% higher increase in apoptotic and necrotic cells when treated with 200 µM Cisplatin than the corresponding control cells. Thus, WRN depleted cells seem to be more sensitive to the crosslinking properties of Cisplatin, supporting a role of WRN in the repair of ICLs (Cheng, Kusumoto, Opresko, Sui, Huang, et al. 2006).

Kp1019 is discussed to be a new promising anticancer drug although the exact mechanisms underlying the cytotoxic effects of KP1019 on tumour cells have not been extensively investigated yet. However, KP1019 is supposed to be able to crosslink DNA as well (KellyJ.M 1990). Although KP1019's crosslinking abilities are supposed to be far beneath those of Cisplatin, the treatment with 100 µM of KP1019 led to a similar decrease of viability as the treatment with 200 µM Cisplatin. This stronger toxicity is presumable not only due to its ICL property but to other yet unknown genotoxic effects or its more specific uptake in cells. KP1019 binds to iron transport proteins and gets into the cell via the transferrin-dependent pathway (Kratz, Hartmann, Keppler, and Messori 1994). Tumour cells, which display a higher iron demand, can therefore be more specifically targeted, making also MDR (multiple drug resistance) tumours susceptible for therapy (Heffeter, Pongratz, Steiner, Chiba, Jakupec, et al. 2005). Additionally, KP1019 is only slightly hindered by the cellular p53 status, which is mutated in at least 50% of human cancers. Our findings show that WRN/KD

cells are more susceptible to KP1019 treatment, suggesting a role of WRN in protecting the cells through its involvement in repair processes.

6.3 Stress response of WRN/SNEV depleted cells

Due to the finding that WRN and SNEV$^{Prp19/Pso4}$ are physically interacting while processing interstrand crosslinks (Zhang, Kaur, Lu, Shen, Li, et al. 2005), we aimed at finding out how a depletion of both proteins could affect the repair of Cisplatin induced ICLs. As expected, the WRN depleted cells showed a lower viability than the controls, confirming WRNs involvement in ICL processing. Surprisingly, the cells lacking SNEV$^{Prp19/Pso4}$ showed a higher survival than the control cells. Cells lacking both proteins, WRN and SNEV$^{Prp19/Pso4}$ showed the highest increase in necrotic/apoptotic cells. This observation could be considered as an additive effect, suggesting WRN and SNEV$^{Prp19/Pso4}$ not to function in the same pathway. Maybe an overexpression of SNEV$^{Prp19/Pso4}$ could restore the repair defects of WRN, or the other way round. This could be an important step to shed light into the interactions of WRN and SNEV$^{Prp19/Pso4}$ considering ICL repair processes. However, this experiment was only performed once and SNEV$^{Prp19/Pso4}$ downregulated cells showed a greater resistance to Cisplatin than the controls. Thus repeating these experiments is absolutely required.

6.4 WRN and splicing

Many findings suggest that SNEV$^{Prp19/Pso4}$, as part of the CDC5L complex (Neubauer, King, Rappsilber, Calvio, Watson, et al. 1998) is an important splicing factor (Tarn, Lee, and Cheng 1993). SNEV$^{Prp19/Pso4}$ is plays an essential role in the second catalytic step in pre-mRNA splicing. As recently reported, SNEV$^{Prp19/Pso4}$ interacts with WRN while processing ICLs and additionally show similar important properties in DNA damage repair, we speculated about a possible role of WRN in splicing as well. We performed a splicing assay in order to compare the alternative splicing pattern of WRN/KD and U2-OS control cells. The WRN depleted cells showed a slightly altered splicing pattern, with an increased amount of 9s splicing product at the expense of the 13s splicing variant. These data indicate a possible role of WRN

in splicing. For confirmation of these data an additional splicing assay, monitoring a WRN overexpressing HeLa cell line was performed as well. Unfortunately, these data don't confirm a role of WRN in alternative splicing at all. Thus, the question whether WRN is involved in the splicing reactions remains to be answered.

7 Appendix

7.1 Abbreviations

AD	deionised water
ATP	adenosine triphosphate
BSO	L-buthionine sulfoximine
CC	coiled-coiled
CMV	cytomegalovirus
CTP	cytosine triphosphate
DAPI	diamidino-2-phenylindol
DdNTP	di-desoxynucleotidtriphsphate
DEPC	diethylpyrocarbonate
DMEM	Dulbecco's Modified Eagle's Medium
DMSO	Dimethylsulfoxid
Ds	double strand
EGFP	enhanced green fluorescent protein
FITC	fluoreszeinisothiocyanate
GTP	guanosintriphosphate
H2O2	Hydrogene peroxide
HEPES	4-(2-hydroxyethyl)-1- piperazineethanesulfonic acid
HR	homologous recombination
HUVEC	human umbilican vein endothelian cell
ICL	inter strand cross links
KD	Knock Down
LP BER	Long Patch Base Exicision Repair
MOPS	3-Morpholinopropanesulfonic acid
NEB	New England Biolabs
NFW	Nuclease Free Water
PAGE	Polyacrylamide Gel Electrophoresis
PCR	Poly chain reaction
PDL	Population Doubling Level
PI	Propidium iodide
Prp19	pre-mRNA processing

PSO4	psoralem sensitivity
RFW	RNase free Water
ROS	Reactive Oxygen Species
SDS	Sodium Dodecylsulfate
SNEV	Sennescence evasion factor
Ss	single strand
TdT	Terminal desoxynucleotidyl Transferase
WRN	Werner
WS	Werner Syndrome

7.2 Materials

SNEV Plasmids

Vectors

PCI neo Invitrogen
PEGFP-C1 Clontech

Polymerase chain reaction (PCR)

dNTPs
GoTaq Polymerase (2500U) (Promega Cat.No. M3178)
GoTaq Buffer 5x (Promega)
NFW (Promega)
Template: 2/3 SNEV Vector (Robin)
Primer (Invitrogen)
Primersequences
SNEV PCI-neo d67 sense (ATTCTCGAGATGCACCACCATCACCACCATgccaccagcatcccggc)
SNEV PCI-neo d91 sense (ATTCTCGAGATGCACCACCATCACCACCATactctgcgccagcagctgc)
SNEV PCI-neo d206 sense (ATTCTCGAGATGCACCACCATCACCACCATaaataccggcaggtggc)
SNEV PCI-neo f.l. sense (ATTCTCGAGATGCACCACCATCACCACCATatgtccctaatctgctcc)
SNEV f.l. a.s. (AtcGAATTCctacaggctgtagaacttg)
SNEV pEGFG-c1 d91 sense (ATTCTCGAGCTactctgcgccagcagctgc)
SNEV pEGFG-c1 f.l. sense (ATTCTCGAGCTatgtccctaatctgctcc)
SNEV pEGFG-c1 206 a.s. (AtcGAATTCgccacctgccggtattt)
SNEV pEGFG-c1 d206 sense(ATTCTCGAGCTaaataccggcaggtggc)
SNEV pEGFG-c1 d67 sense (ATTCTCGAGCTgccaccagcatcccggc)
PCR cycler

DNA purification after PCR and Gel cleanup
PCR Wizard SV Gel and PCR Clean-Up System, Promega, A9282

<u>Quantification of DNA</u>
<u>Agarose Gel</u>
1% Agarose
Ethidium bromide 10 mg/ml, (Fermentas)
TAE-Buffer 50× stock solution
242 g Tris base
57.1 ml glacial acetic acid
37.2 g $Na_2EDTA\ 2H_2O$
H_2O to 1 liter pH 8.5:
λ DNA / EcoRI, HIND III-Marker 3 (Fermentas SM0191/2/3)
6x Loading Dye (Fermentas)
UV-scanner
Gel chamber

Power supply
Photometric Quantisiation
BioPhotometer (Eppendorf, Hamburg, Germany)
UVette® cuvettes

Bioanalyzer

DNA 1000 Kit 5067-1504 (Agilent Life Science)
DNA 1000 Lab chip
DNA Ladder Mix
Loading dye
Gel mix
Chip station
Shaker
Bioanalyzer 2100 Software
Agilent 2100 electrophoresis bioanalyzer (Agilent Life Science)

Restriction

ECORI (10U/µl) NEB (New England Biolabs)
ECORI Buffer (NEB)
BSA (NEB)
XHOI (10U/µl) (NEB)
NFW (Promega)
Heating Block

Ligation

T4 DNA Ligase (400.000U/ml) (NEB Cat.No.M0202S)
T4 DNA Ligase Reaction Buffer 10x (NEB)
Nuclease free water (Promega)

Electroporation

Electrocompetent E.coli, DH10B
1 mM HEPES 4- (2-Hydroxyethyl-1piperazinethanesulfanesulfic acid buffer)
10 % glycerol (autoclaved)
87 % glycerol (autoclaved)
prechilled 1 ml Eppendorf tubes
Liquid nitrogen

Precipitation of DNA

Ethanol 96%
2, 5 M Natrium Acetate Merck pH 5,2
Gene Pulser (Biorad)

Media

SOC Medium
- 0.5% Yeast Extract
- 10 mM NaCl
- 2.5 mM KCl
- 10 mM $MgCl_2$
- 20 mM Glucose
- 20 mM $MgSO_4$
- 2.0% Trypton

LB-Medium (1L)
- 10 g Peptone from casein
- 5 g Yeast
- 10 g NaCl

LB-Agar (1L)
- 10 g Peptone from casein
- 5 g Yeast
- 10 g NaCl

15g Agar
Media should reach pH 7
Media should be autoclaved shortly after preparation

Antibiotics

LB-Amp
- Ampicillin (100 mg/ml) stored at -20°C
- 100 µl of Ampicillin is added to 100 ml of LB-Medium.

LB-Kan
- Kanamycin (100 mg/ml) stored at -20°C
- 100 µl of Ampicillin is added to 100 ml of LB-Medium.

Storage of antibiotic containing media at 4°C.

PCR screening of Positive clones
Primer:
for pEGFP-c:
EGFP End sense
sv40 polyA a s;
for: pCI-neo:
T3 sense AAGCATTAACCCTCACTAAAGG
T7 pCI a.s ACTTAATACGACTCACTATAGGT3
dNTPs
GoTaq Polymerase (2500U)(Promega Cat.No.M3178)
GoTaq Buffer 5x (Promega)
NFW (Promega)
PCR cycler

Miniprep
Wizard® Plus SV Minipreps DNA Purification System Cat. No: A1330 (Promega GmbH, Mannheim, Germany)

Cell Resuspension Solution 50mM Tris-HCl (pH 7.5) 10mM EDTA 100µg/ml RNase A
Cell Lysis Solution 0.2M NaOH 1% SDS
Neutralization Solution 1.32M potassium acetate (pH 4.8)
Column Wash Solution 80mM potassium acetate 8.3mM Tris-HCl (pH 7.5) 40µM EDTA Add 95% ethanol to a final ethanol concentration of about 55%.

Sequencing
Performed by Martin IBL, Vienna

Endofree maxiprep
Endotoxin Free Maxi Prep Cat. No: 12362 (Quiagen)
Buffer P1 (Resuspension buffer) 10 mM EDTA, 50 mM Tris·Cl, pH 8.0; addition of 100 µg/ml RNase A
Buffer P2 (Lysis buffer) 200 mM NaOH, 1% SDS (w/v)
Buffer P3 (Neutralization buffer) 3.0 M potassium acetate
Buffer QBT (Equilibration buffer) 750 mM NaCl, 50 mM MOPS, pH 7.0; 15% isopropanol (v/v); 0.15% Triton® X-100 (v/v)
Buffer QC (Wash buffer) 1.0 M NaCl, 50 mM MOPS, pH 7.0; 15% isopropanol (v/v)
Buffer QN (Elution buffer) 1.6 M NaCl, 15–25°C 50 mM MOPS, pH 7.0; 15% isopropanol (v/v)
TE 10 mM Tris·Cl, pH 8.0, 1 mM EDTA
(all reagents supplied by Quiagen)
Endotoxin-free 70% ethanol (add 40 ml of 96–100% ethanol to the endotoxin-free water supplied with the kit)
Isopropanol

Cell culture

HeLa
Culture Medium
RPMI Medium (Dulbecco Biochrom AG, Berlin Germany)
4mM L-Glutamin
10% FCS (Hyclone)
0,1% Trypsin/EDTA
- 9,55 PBS
- 1g Trypsin
- 0,2g EDTA-Na_4*$2H_2O$
- Pyrogene free AD

Autoclaved, aliquoted and stored at -20°C
PBS def pH 7, 2 +/- 0, 1 pyrogenfree (Dulbecco Biochrom AG, Berlin Germany)
Holten Laminair HBB2448
Incubaor
- Hera Cell
- Espec BNA-311

U2-OS
Culture Medium
DMEM Medium (Dulbecco Biochrom AG, Berlin Germany)
4mM L-Glutamin
10% FCS (Hyclone)
200µg/ml Hygromycin
0,25% Trypsin/EDTA
- 9,55 PBS
- 2,5g Trypsin
- 0,2g EDTA-Na_4*$2H_2O$

Pyrogene free AD
Autoclaved, aliquoted and stored at -20°C
PBS def pH 7,2 +/- 0,1 pyrogenfree (Dulbecco, biochrom AG, Berlin Germany)
Holten Laminair HBB2448
Incubaor
Hera Cell
Espec BNA-311

Calculation of cell number
0, 5% TryphanBlue in PBS def.
Bürker Türck counting chambers
Microscope Olympus CK2

Cryopreservation
Cryo medium
10% FCS
10% DMSO (D260, Sigma)
In culture medium
1,8ml Cryotubes
10ml Centrifugation tubes
Sigma laboratory centrifuge 93387
Liquid Nitrogen

Mycoplasma test
200µl DAPI (5mg/ml) in 10ml cold Methanol
PBS def. (Dulbecco, biochrom AG, Berlin Germany)
Fluoroprep mounting medium (Biomerieux, Marcy d'Etoile, France)
Chamber Slides™ (Nunc, Wiesbaden, Germany)
Confocal microscope BH-2-RFCA (Olympus, Hamburg, Germany)

Lipofection
Lipofectamin™ 2000 (Invitrogen)
Opti-MEM® I reduced serum Medium (Invitrogen,31985-062)
siRNA
20pmol/µl On TARGETplus siRNA WRN (human) (Dharmacon Cat.No: J-010378-05)
20pmol/µl On TARGETplus siRNA SNEV (human) Dharmacon Cat.No: J-004668-05
20pmol/µl non targeting (Dharmacon Cat.No: D-001210-02-20)
5nmol diluted in 250µl siRNA buffer (Dharmacon), aliquoted and stored at -80°C

Nucleofection
Cell Nucleofector® transfection Kit V (Amaxa biosystems, USA)
Nucleofector® (Amaxa biosystems, USA)
Nucleofection Cuvettes (Amaxa biosystems, USA)

Protein characterisation

Protein harvest
Lysis buffer (NE)
50mM Tris pH 7,5
0,5m nAcL
1% Sodiumdeoxycholate
0,1% SDS
2mM EDTA
1 tablet Complete protease Inhibitor
AD
Centrifuge 5451 (Eppendorf Hamburg Germany)
QIAE-shredder Mini columns (Qiagen)
Liquid Nitrogen

Bradford
BioRad Bradford reagent
Dilution buffer
6,80g KH2PO4
8,76g NaCl
AD
Set pH to 7, 2 with KOH
96 well dilution plates
Sunrise Reader (Tecan)
Magellan software

SDS-PAGE

2x SDS Sample Buffer
- 2,5 ml 0,5M Tris pH 6,8
- 2ml Glycerol
- 4ml SDS 10%
- 0,1mg Bromphenol Blue
- DTT
- AD

Sea Blue Plus 2 (Invitrogen, Cat. No.LC5929)
NuPAGE® Bis-Tris Gels (4-12%) (Invitrogen)
NuPAGE MOPS SDS-running buffer 20 x (Invitrogen)
40 ml NuPAGE MOPS SDS-running buffer 20x were diluted with A.D. to a final volume of 800 ml.
XCell *SureLock*™ Mini Cell gel caster (Invitrogen)
Power supply
Geltips (Biorad)

Western Blotting

PVDF membrane
XCell *SureLock*™ Mini Cell gel caster (Invitrogen)
Power supply
1 x Transfer Buffer 1L
- 50ml 20x NuPage transfer buffer Invitrogen
- 100 ml Methanol Roth
- AD

Blocking Buffer
3% Skim Milk Powder dissolved in 0.1% TPBS
0,1% TPBS (washing Buffer) 1L
- 8,0g NaCl
- 0,2g KCl
- 1,15g Na_2HpO_4
- 0,2g KH_2PO_4
- AD
- 1ml Triton X-100 Sigma

Adjust to pH 7, 4 with HCl
Antibody
- Anti-WRN Santa Cruz (H-300)sc-5629
- primary 1:1000 in blocking buffer
- Anti-Rabbit IgG (Conjugate) HRP Sigma A0545-1ML
- Secondary 1:10.000 in Blocking Buffer
- Anti-SNEV prp19 688
- Primary 1:2.500 in 0,1% TPBS
- Ant-ß-Actin Sigma A-5441
- Primary 1:5.000 in blocking buffer
- Anti Mouse IgG (y-chain specific) HRP Sigma A3673-1ML
- Secondary 1:10.000 in blocking buffer

Chemiluminsecence

Chemiluminescent Peroxidase Substrate for Western Blotting, Sigma CPS-1-120
Typhoon 9400 Amersham Bioscience
Image Quant software Amersham Bioscience

Silver stain

Fixation solution 1L
- 500 ml Ethanol
- 100ml acetic acid
- AD

Incubation solution 1L
- 150ml Ethanol
- 34g Sodium acetate
- 1g Na_2S2O_3
- AD

Add 62,5µl glutaraldehyde (50%) to 25 ml immediately before use
$AgNO_3$ Solution 500 ml
0,5g $AgNO_3$
Add 10µl Formaldehyde to 25ml immediately before use
Developer Solution 500ml
- 12, 5 g Na_2CO_3
- AD

Add 2, 5µl Formaldehyde to 25ml immediately before use
Stop-solution 500ml
- 7,3g EDTA
- AD

Conservation solution 500ml

50ml Glycerol (87%)
AD

RNA characterisation

RNA isolation

RNA isolation using RNeasy kit

RNeasy Mini Kit (50) (Quiagen) Cat.No: 74104
RNeasy Mini Spin Columns (pink) Collection Tubes (1.5 ml) 50 250
Collection Tubes (2 ml)
Buffer RLT
Buffer RW1
Buffer RPE (concentrate) 11 ml + 44ml 96% - 100% ethanol
55 ml RNase-Free Water
RNase-Free DNase Set 79254
DNase I, RNase-Free (lyophilized) 1500 U
Buffer RDD
RNase-Free Water
DNAse I stock solution: inject 550 µl RNase-free water into the DNase I vial and mix gently by inverting the vial. Aliquotes stored at -20°C
DNAse solution: ad 10µl of DNAseI stock solution to 70µl RDD Buffer
QIAshredder (Quiagen Cat.No. 79656)
Eppendorf centrifuge

RNA isolation with Trizol

Trizol (Invitrogen)
RNase free Sarstedt tubes
Chloroform
Isopropanol
70% Ethanol (96% Ethanol in RFW)
RFW (Promega)
Eppendorf centrifuge cooled

RNA quantisation

Photometric

BioPhotometer (Eppendorf, Hamburg, Germany)
UVette® cuvettes
AD

Bioanalyzer

RNA 6000 nano Kit 5067 1511 (Agilent Life Science)
RNA nano Lab chip
RNA Ladder Mix
Loading dye (adding 1µl of RNA 6000 Nano dye concentrate with 65µl of filtered gel aliquots)
Gel mix
Chip station
shaker
Bioanalyzer 2100 Software
Agilent 2100 electrophoresis bioanalyzer (Agilent Life Science)

Agarose Gel

Gel

1,2g Agarose
90ml DEPC Water
12ml MOPS 10x
19,8ml Formaldehyde p.A. (37%)
RNA 2x dye (Ambion)
RNA ladder (Fermentas)
Fume Hood
UV-scanner

Reverse transcription

SuperScript III RT (10000U) (Invitrogen Cat. No 18080-044)
First strand Buffer (5x) (Invitrogen)
0,1M DTT
RNase OUT (5000U) (Invitrogen Cat. No 10777-019)
Oligo$(dT)_{18}$ primer
dNTPs
NFW (Promega)
Heating Block
Eppendorf centrifuge

Real Time PCR

Platinum®Sybr®Green qPCR SuperMix-UDG (Invitrogen, Cat.No.11733038)
WRN RT (1)
Sense TTTCCATCTTTGCCATCATCATCTTTA
a.s.AAGTCATTACGGTGTCCTA
WRN RT (2)
SenseGACTCGTCTTCTGTGTTCTTCTTGA
a.s. TTGAAAACGTAAAAAGGATTGAT
SNEV RT primer:
Sense AACCACGGAGCGCAAGAAG
A s CGGGGGAAGCAGAAAACAC
GAPDH primer
Sense TGCACCACCAACTGCTTAGC
As GGCATGGACTGTGGTCATGAG
AD
Rotor Gene 2000 Real time Cycler (Corbett Research)

Stress

Stressing reagents
H_2O_2: Hydrogeneperoxide 3% (Sigma, H6520)
Cisplatin: Cis- diamminePlatinum (II) dichloride (Keppler, Insitute of Inorganic Chemistry, Vienna)
Bleomycine: Bleomycin sulphate (sigma, B5507)
BSO: DL-buthionine –[S,R] – sulfoximine (Sigma, B2640)
KP1019: indazolium *trans*-[tetrachlorobis(1*H*-indazole)ruthenate(III)] (Keppler, Insitute of Inorganic Chemistry, Vienna)
DMSO (D260, Sigma)

Apoptosis assay
PBS def pH 7, 2 +/- 0, 1 pyrogenfree (Dulbecco Biochrom AG, Berlin Germany)
Trypsin 0,25% (0,02%EDTA)
FCS (Hyclon)
PI (Merck)
Annexin V- FLUOS (Roche Diagnostic GmbH, Mannheim, Germany, Cat. No: 1 828 81)
Annexin V binding Buffer
10MHEPES/NaOH pH 7, 4
140mM NaCl
5mM $CaCl_2$
Annexin V/PI incubation Buffer
250ng/ml PI
20µl/ml Annexin V -FLUOS
Diluted in Annexin V binding Buffer
FACS-calibur (Becton Dickson, franklin lakes, NJ, USA)
Cell Quest software (Becton Dickson, franklin lakes, NJ, USA)
10ml FACS tubes

7.3 References

Ajuh, P., B. Kuster, K. Panov, J. C. Zomerdijk, M. Mann, and A. I. Lamond
2000 Functional analysis of the human CDC5L complex and identification of its components by mass spectrometry. *Embo J* 19: 6569-81.

Allsopp, R. C., H. Vaziri, C. Patterson, S. Goldstein, E. V. Younglai, A. B. Futcher, C. W. Greider, and C. B. Harley
1992 Telomere length predicts replicative capacity of human fibroblasts. *Proc Natl Acad Sci U S A* 89: 10114-8.

Aravind, L., and E. V. Koonin
2000 The U box is a modified RING finger - a common domain in ubiquitination [letter]. *Curr Biol* 10: R132-4.

Beausejour, C. M., A. Krtolica, F. Galimi, M. Narita, S. W. Lowe, P. Yaswen, and J. Campisi
2003 Reversal of human cellular senescence: roles of the p53 and p16 pathways. *Embo J* 22: 4212-22.

Blackburn, E. H.
2005 Telomeres and telomerase: their mechanisms of action and the effects of altering their functions. *FEBS Lett* 579: 859-62.

Bodnar, A. G., M. Ouellette, M. Frolkis, S. E. Holt, C. P. Chiu, G. B. Morin, C. B. Harley, J. W. Shay, S. Lichtsteiner, and W. E. Wright
1998 Extension of life-span by introduction of telomerase into normal human cells [see comments]. *Science* 279: 349-52.

Brosh, R. M., Jr., C. von Kobbe, J. A. Sommers, P. Karmakar, P. L. Opresko, J. Piotrowski, I. Dianova, G. L. Dianov, and V. A. Bohr
2001 Werner syndrome protein interacts with human flap endonuclease 1 and stimulates its cleavage activity. *Embo J* 20: 5791-801.

Chang, M. W., J. Grillari, C. Mayrhofer, K. Fortschegger, G. Allmaier, G. Marzban, H. Katinger, and R. Voglauer
2005 Comparison of early passage, senescent and hTERT immortalized endothelial cells. *Exp Cell Res* 309: 121-36.

Chen, Q., A. Fischer, J. D. Reagan, L. J. Yan, and B. N. Ames
1995 Oxidative DNA damage and senescence of human diploid fibroblast cells. *Proc Natl Acad Sci U S A* 92: 4337-41.

Cheng, S. C., W. Y. Tarn, T. Y. Tsao, and J. Abelson
1993 PRP19: a novel spliceosomal component. *Mol Cell Biol* 13: 1876-82.

Cheng, W. H., R. Kusumoto, P. L. Opresko, X. Sui, S. Huang, M. L. Nicolette, T. T. Paull, J. Campisi, M. Seidman, and V. A. Bohr
2006 Collaboration of Werner syndrome protein and BRCA1 in cellular responses to DNA interstrand cross-links. *Nucleic Acids Res* 34: 2751-60.

Choi, H. S., Z. Lin, B. S. Li, and A. Y. Liu
1990 Age-dependent decrease in the heat-inducible DNA sequence-specific binding activity in human diploid fibroblasts. *J Biol Chem* 265: 18005-11.

Cooper, M. P., A. Machwe, D. K. Orren, R. M. Brosh, D. Ramsden, and V. A. Bohr
2000 Ku complex interacts with and stimulates the Werner protein. *Genes Dev* 14: 907-12.

Cristofalo, V. J., and R. J. Pignolo
1993 Replicative senecence of human fibroblast-like cells in culture. *Physiol Rev* 73: 617-38.

d'Adda di Fagagna, F., P. M. Reaper, L. Clay-Farrace, H. Fiegler, P. Carr, T. Von Zglinicki, G. Saretzki, N. P. Carter, and S. P. Jackson
2003 A DNA damage checkpoint response in telomere-initiated senescence. *Nature* 426: 194-8. Epub 2003 Nov 5.

Deckert, J., K. Hartmuth, D. Boehringer, N. Behzadnia, C. L. Will, B. Kastner, H. Stark, H. Urlaub, and R. Luhrmann
2006 Protein composition and electron microscopy structure of affinity-purified human spliceosomal B complexes isolated under physiological conditions. *Mol Cell Biol* 26: 5528-43.

Di Leonardo, A., S. P. Linke, K. Clarkin, and G. M. Wahl
1994 DNA damage triggers a prolonged p53-dependent G1 arrest and long-term induction of Cip1 in normal human fibroblasts. *Genes Dev* 8: 2540-51.

Dickson, M. A., W. C. Hahn, Y. Ino, V. Ronfard, J. Y. Wu, R. A. Weinberg, D. N. Louis, F. P. Li, and J. G. Rheinwald

2000 Human keratinocytes that express hTERT and also bypass a p16(INK4a)- enforced mechanism that limits life span become immortal yet retain normal growth and differentiation characteristics. *Mol Cell Biol* 20: 1436-47.

Dimri, G. P., X. Lee, G. Basile, M. Acosta, G. Scott, C. Roskelley, E. E. Medrano, M. Linskens, I. Rubelj, O. Pereira-Smith, and et al.
1995 A biomarker that identifies senescent human cells in culture and in aging skin in vivo. *Proc Natl Acad Sci U S A* 92: 9363-7.

Eller, M. S., X. Liao, S. Liu, K. Hanna, H. Backvall, P. L. Opresko, V. A. Bohr, and B. A. Gilchrest
2006 A role for WRN in telomere-based DNA damage responses. *Proc Natl Acad Sci U S A* 103: 15073-8.

Erusalimsky, J. D., and D. J. Kurz
2005 Cellular senescence in vivo: its relevance in ageing and cardiovascular disease. *Exp Gerontol* 40: 634-42.

Foreman, P. K., and J. L. Hamlin
1989 Identification and characterization of a gene that is coamplified with dihydrofolate reductase in a methotrexate-resistant CHO cell line. *Mol Cell Biol* 9: 1137-47.

Fortschegger, K., B. Wagner, R. Voglauer, H. Katinger, M. Sibilia, and J. Grillari
2007 Early Embryonic Lethality of Mice Lacking the Essential Protein SNEV. *Mol Cell Biol.*

Fuertesa, M. A., J. Castillab, C. Alonsoa, and J. M. Perez
2003 Cisplatin biochemical mechanism of action: from cytotoxicity to induction of cell death through interconnections between apoptotic and necrotic pathways. *Curr Med Chem* 10: 257-66.

Fujiwara, Y., T. Higashikawa, and M. Tatsumi
1977 A retarded rate of DNA replication and normal level of DNA repair in Werner's syndrome fibroblasts in culture. *J Cell Physiol* 92: 365-74.

Giaever, G., A. M. Chu, L. Ni, C. Connelly, L. Riles, S. Veronneau, S. Dow, A. Lucau-Danila, K. Anderson, B. Andre, A. P. Arkin, A. Astromoff, M. El-Bakkoury, R. Bangham, R. Benito, S. Brachat, S. Campanaro, M. Curtiss, K. Davis, A. Deutschbauer, K. D. Entian, P. Flaherty, F. Foury, D. J. Garfinkel, M. Gerstein, D. Gotte, U. Guldener, J. H. Hegemann, S. Hempel, Z. Herman, D. F. Jaramillo, D. E. Kelly, S. L. Kelly, P. Kotter, D. LaBonte, D. C. Lamb, N. Lan, H. Liang, H. Liao, L. Liu, C. Luo, M. Lussier, R. Mao, P. Menard, S. L. Ooi, J. L. Revuelta, C. J. Roberts, M. Rose, P. Ross-Macdonald, B. Scherens, G. Schimmack, B. Shafer, D. D. Shoemaker, S. Sookhai-Mahadeo, R. K. Storms, J. N. Strathern, G. Valle, M. Voet, G. Volckaert, C. Y. Wang, T. R. Ward, J. Wilhelmy, E. A. Winzeler, Y. Yang, G. Yen, E. Youngman, K. Yu, H. Bussey, J. D. Boeke, M. Snyder, P. Philippsen, R. W. Davis, and M. Johnston
2002 Functional profiling of the Saccharomyces cerevisiae genome. *Nature* 418: 387-91.

Goldstein, S.
1990 Replicative senescence: the human fibroblast comes of age. *Science* 249: 1129-33.

Gonczy, P., C. Echeverri, K. Oegema, A. Coulson, S. J. Jones, R. R. Copley, J. Duperon, J. Oegema, M. Brehm, E. Cassin, E. Hannak, M. Kirkham, S. Pichler, K. Flohrs, A. Goessen, S. Leidel, A. M. Alleaume, C. Martin, N. Ozlu, P. Bork, and A. A. Hyman
2000 Functional genomic analysis of cell division in C. elegans using RNAi of genes on chromosome III. *Nature* 408: 331-6.

Greider, C. W., and E. H. Blackburn
1985 Identification of a specific telomere terminal transferase activity in Tetrahymena extracts. *Cell* 43: 405-13.

Griffith, J. D., L. Comeau, S. Rosenfield, R. M. Stansel, A. Bianchi, H. Moss, and T. de Lange
1999 Mammalian telomeres end in a large duplex loop. *Cell* 97: 503-14.

Grillari, J., P. Ajuh, G. Stadler, M. Loscher, R. Voglauer, W. Ernst, J. Chusainow, F. Eisenhaber, M. Pokar, K. Fortschegger, M. Grey, A. I. Lamond, and H. Katinger

2005 SNEV is an evolutionarily conserved splicing factor whose oligomerization is necessary for spliceosome assembly. *Nucleic Acids Res* 33: 6868-83.

Grillari, J., O. Hohenwarter, R. M. Grabherr, and H. Katinger
2000 Subtractive hybridization of mRNA from early passage and senescent endothelial cells. *Exp Gerontol* 35: 187-97.

Grillari, Voglauer
2007 Prp19. *Targeted Proteins Database,* http://www.currentbiodata.com/productsHbdp.htm.

Hahn, W. C., S. A. Stewart, M. W. Brooks, S. G. York, E. Eaton, A. Kurachi, R. L. Beijersbergen, J. H. Knoll, M. Meyerson, and R. A. Weinberg
1999 Inhibition of telomerase limits the growth of human cancer cells. *Nat Med* 5: 1164-70.

Harley, C. B.
1991 Telomere loss: mitotic clock or genetic time bomb? *Mutat Res* 256: 271-82.

Harrigan, J. A., and V. A Bohr
2003 Human diseases deficient in RecQ helicases. *Biochimie* 85: 1185-93.

Harrigan JA, Wilson DM 3rd, Prasad R, Opresko PL, Beck G, May A, Wilson SH, Bohr VA.
2006 The Werner syndrome protein operates in base excision repair and cooperates with DNA polymerase beta. *Nucleic Acids Res* 30: 745-54.

Harrington, L., and M. O. Robinson
2002 Telomere dysfunction: multiple paths to the same end. *Oncogene* 21: 592-7.

Hatakeyama, S., M. Yada, M. Matsumoto, N. Ishida, and K. I. Nakayama
2001 U-Box proteins as a new family of ubiquitin-protein ligases. *J Biol Chem* 276: 33111-33120.

Haupt, S., M. Berger, Z. Goldberg, and Y. Haupt
2003 Apoptosis - the p53 network. *J Cell Sci* 116: 4077-85.

Hayflick, L. , and P.S. Moorhead
1961 The serial cultivation of human diploid cell strains. *Exp Cell Res* 25: 585-621.

Heffeter, P., M. Pongratz, E. Steiner, P. Chiba, M. A. Jakupec, L. Elbling, B. Marian, W. Korner, F. Sevelda, M. Micksche, B. K. Keppler, and W. Berger
2005 Intrinsic and acquired forms of resistance against the anticancer ruthenium compound KP1019 [indazolium trans-[tetrachlorobis(1H-indazole)ruthenate (III)] (FFC14A). *J Pharmacol Exp Ther* 312: 281-9.

Heydari, A. R., B. Wu, R. Takahashi, R. Strong, and A. Richardson
1993 Expression of heat shock protein 70 is altered by age and diet at the level of transcription. *Mol Cell Biol* 13: 2909-18.

Hofseth, L. J., S. P. Hussain, and C. C. Harris
2004 p53: 25 years after its discovery. *Trends Pharmacol Sci* 25: 177-81.

Horikoshi, T., A. K. Balin, and D. M. Carter
1991 Effects of oxygen tension on the growth and pigmentation of normal human melanocytes. *J Invest Dermatol* 96: 841-4.

Jiao R, Harrigan JA, Shevelev I, Dietschy T, Selak N, Indig FE, Piotrowski J, Janscak P, Bohr VA, Stagljar I.
2006 The Werner syndrome protein is required for recruitment of chromatin assembly factor 1 following DNA damage. *Oncogene advanced online publication* 18.

Kapitza, S., M. A. Jakupec, M. Uhl, B. K. Keppler, and B. Marian

2005 The heterocyclic ruthenium(III) complex KP1019 (FFC14A) causes DNA damage and oxidative stress in colorectal tumor cells. *Cancer Lett* 226: 115-21.

Karlseder, J., D. Broccoli, Y. Dai, S. Hardy, and T. de Lange
1999 p53- and ATM-dependent apoptosis induced by telomeres lacking TRF2. *Science* 283: 1321-5.

KellyJ.M, . FeeneM.M, . Tossi A.B, J.P. Lecomte and A. Kirsch-De Mesmaeker,
1990 Interaction of tetra-azaphenanthrene ruthenium complexes with DNA and oligonucleotides. A photophysical and photochemical investigation. *Anticancer Drug Des* 5: 69-75.

Kiyono, T., S. A. Foster, J. I. Koop, J. K. McDougall, D. A. Galloway, and A. J. Klingelhutz
1998 Both Rb/p16INK4a inactivation and telomerase activity are required to immortalize human epithelial cells [see comments]. *Nature* 396: 84-8.

Kratz, F., M. Hartmann, B. Keppler, and L. Messori
1994 The binding properties of two antitumor ruthenium(III) complexes to apotransferrin. *J Biol Chem* 269: 2581-8.

Krtolica, A., S. Parrinello, S. Lockett, P. Y. Desprez, and J. Campisi
2001 Senescent fibroblasts promote epithelial cell growth and tumorigenesis: a link between cancer and aging. *Proc Natl Acad Sci U S A* 98: 12072-7.

Loscher, M., K. Fortschegger, G. Ritter, M. Wostry, R. Voglauer, J. A. Schmid, S. Watters, A. J. Rivett, P. Ajuh, A. I. Lamond, H. Katinger, and J. Grillari
2005 Interaction of U-box E3 ligase SNEV with PSMB4, the beta7 subunit of the 20 S proteasome. *Biochem J* 388: 593-603.

Mahajan, K. N., and B. S. Mitchell
2003 Role of human Pso4 in mammalian DNA repair and association with terminal deoxynucleotidyl transferase. *Proc. Natl. Acad. Sci. USA* 100: 10746-51.

Makarov, E. M., O. V. Makarova, H. Urlaub, M. Gentzel, C. L. Will, M. Wilm, and R. Luhrmann
2002 Small nuclear ribonucleoprotein remodeling during catalytic activation of the spliceosome. *Science* 298: 2205-8.

Makarova, O. V., E. M. Makarov, H. Urlaub, C. L. Will, M. Gentzel, M. Wilm, and R. Luhrmann
2004 A subset of human 35S U5 proteins, including Prp19, function prior to catalytic step 1 of splicing. *Embo J* 23: 2381-91.

Martin, G. M.
1999 What geriatricians should know about the Werner syndrome. *J Am Geriatr Soc* 47: 1136-44.

Milchanowski, A. B., A. L. Henkenius, M. Narayanan, V. Hartenstein, and U. Banerjee
2004 Identification and characterization of genes involved in embryonic crystal cell formation during Drosophila hematopoiesis. *Genetics* 168: 325-339.

Minamino, T., and I. Komuro
2007 Vascular cell senescence: contribution to atherosclerosis. *Circ Res* 100: 15-26.

Mushegian, A. R., D. E. Bassett, Jr., M. S. Boguski, P. Bork, and E. V. Koonin
1997 Positionally cloned human disease genes: patterns of evolutionary conservation and functional motifs. *Proc Natl Acad Sci U S A* 94: 5831-6.

Neubauer, G., A. King, J. Rappsilber, C. Calvio, M. Watson, P. Ajuh, J. Sleeman, A. Lamond, and M. Mann
1998 Mass spectrometry and EST-database searching allows characterization of the multi-protein spliceosome complex. *Nat Genet* 20: 46-50.

Nir-Paz, R., M. C. Prevost, P. Nicolas, A. Blanchard, and H. Wroblewski
2002 Susceptibilities of Mycoplasma fermentans and Mycoplasma hyorhinis to membrane-active peptides and enrofloxacin in human tissue cell cultures. *Antimicrob Agents Chemother* 46: 1218-25.

Ohi, M. D., C. W. Vander Kooi, J. A. Rosenberg, W. J. Chazin, and K. L. Gould
2003 Structural insights into the U-box, a domain associated with multi- ubiquitination. *Nat Struct Biol* 10: 250-255.

Olovnikov, A. M.
1973 A theory of marginotomy. The incomplete copying of template margin in enzymic synthesis of polynucleotides and biological significance of the phenomenon. *J Theor Biol* 41: 181-90.

Oshima, J., C. E. Yu, M. Boehnke, J. L. Weber, S. Edelhoff, M. J. Wagner, D. E. Wells, S. Wood, C. M. Disteche, G. M. Martin, and et al.
1994 Integrated mapping analysis of the Werner syndrome region of chromosome 8. *Genomics* 23: 100-13.

Otterlei, M., P. Bruheim, B. Ahn, W. Bussen, P. Karmakar, K. Baynton, and V. A. Bohr
2006 Werner syndrome protein participates in a complex with RAD51, RAD54, RAD54B and ATR in response to ICL-induced replication arrest. *J Cell Sci.*

Parrinello, S., J. P. Coppe, A. Krtolica, and J. Campisi
2005 Stromal-epithelial interactions in aging and cancer: senescent fibroblasts alter epithelial cell differentiation. *J Cell Sci* 118: 485-96.

Poot, M., H. Hoehn, T. M. Runger, and G. M. Martin
1992 Impaired S-phase transit of Werner syndrome cells expressed in lymphoblastoid cell lines. *Exp Cell Res* 202: 267-73.

Rodier, F., S. H. Kim, T. Nijjar, P. Yaswen, and J. Campisi
2005 Cancer and aging: the importance of telomeres in genome maintenance. *Int J Biochem Cell Biol* 37: 977-90.

Rodriguez-Lopez, A. M., D. A. Jackson, F. Iborra, and L. S. Cox
2002 Asymmetry of DNA replication fork progression in Werner's syndrome. *Aging Cell* 1: 30-9.

Rufer, N., M. Migliaccio, J. Antonchuk, R. K. Humphries, E. Roosnek, and P. M. Lansdorp
2001 Transfer of the human telomerase reverse transcriptase (TERT) gene into T lymphocytes results in extension of replicative potential. *Blood* 98: 597-603.

Salk, D.
1982 Can we learn about aging from a study of Werner's syndrome? *J Am Geriatr Soc* 30: 334-9.

Satyanarayana, A., S. U. Wiemann, J. Buer, J. Lauber, K. E. Dittmar, T. Wustefeld, M. A. Blasco, M. P. Manns, and K. L. Rudolph
2003 Telomere shortening impairs organ regeneration by inhibiting cell cycle re-entry of a subpopulation of cells. *Embo J* 22: 4003-13.

Serrano, M., A. W. Lin, M. E. McCurrach, D. Beach, and S. W. Lowe
1997 Oncogenic ras provokes premature cell senescence associated with accumulation of p53 and p16INK4a. *Cell* 88: 593-602.

Spillare, E. A., A. I. Robles, X. W. Wang, J. C. Shen, C. E. Yu, G. D. Schellenberg, and C. C. Harris
1999 p53-mediated apoptosis is attenuated in Werner syndrome cells. *Genes Dev* 13: 1355-60.

Stanulis-Praeger, B. M.
1987 Cellular senescence revisited: a review. *Mech Ageing Dev* 38: 1-48.

Szekely, A. M., F. Bleichert, A. Numann, S. Van Komen, E. Manasanch, A. Ben Nasr, A. Canaan, and S. M. Weissman
2005 Werner protein protects nonproliferating cells from oxidative DNA damage. *Mol Cell Biol* 25: 10492-506.

Tarn, W. Y., K. R. Lee, and S. C. Cheng
1993 Yeast precursor mRNA processing protein PRP19 associates with the spliceosome concomitant with or just after dissociation of U4 small nuclear RNA. *Proc Natl Acad Sci U S A* 90: 10821-5.

TerBush, D. R., T. Maurice, D. Roth, and P. Novick
1996 The Exocyst is a multiprotein complex required for exocytosis in Saccharomyces cerevisiae. *Embo J* 15: 6483-94.

Toussaint, O., P. Dumont, J. Remacle, J. F. Dierick, T. Pascal, C. Frippiat, J. P. Magalhaes, S. Zdanov, and F. Chainiaux
2002 Stress-induced premature senescence or stress-induced senescence-like phenotype: one in vivo reality, two possible definitions? *ScientificWorldJournal* 2: 230-47.

Voglauer, R., M. W. Chang, B. Dampier, M. Wieser, K. Baumann, T. Sterovsky, M. Schreiber, H. Katinger, and J. Grillari
2006 SNEV overexpression extends the life span of human endothelial cells. *Exp Cell Res* 312: 746-59.

Wang, E.
1995 Senescent human fibroblasts resist programmed cell death, and failure to suppress bcl2 is involved. *Cancer Res* 55: 2284-92.

West, M. D., O. M. Pereira-Smith, and J. R. Smith
1989 Replicative senescence of human skin fibroblasts correlates with a loss of regulation and overexpression of collagenase activity. *Exp Cell Res* 184: 138-47.

Yang, X., M. R. Bani, S. J. Lu, S. Rowan, Y. Ben-David, and B. Chabot
1994 The A1 and A1B proteins of heterogeneous nuclear ribonucleoparticles modulate 5' splice site selection in vivo. *Proc Natl Acad Sci U S A* 91: 6924-8.

Yu, C. E., J. Oshima, Y. H. Fu, E. M. Wijsman, F. Hisama, R. Alisch, S. Matthews, J. Nakura, T. Miki, S. Ouais, G. M. Martin, J. Mulligan, and G. D. Schellenberg
1996 Positional cloning of the Werner's syndrome gene. *Science* 272: 258-62.

Zhang, N., R. Kaur, X. Lu, X. Shen, L. Li, and R. J. Legerski
2005 The Pso4 mRNA splicing and DNA repair complex interacts with WRN for processing of DNA interstrand cross-links. *J Biol Chem* 280: 40559-67.

Zhang, X., V. Mar, W. Zhou, L. Harrington, and M. O. Robinson
1999 Telomere shortening and apoptosis in telomerase-inhibited human tumor cells. *Genes Dev* 13: 2388-99.

Zhu, J., H. Wang, J. M. Bishop, and E. H. Blackburn
1999 Telomerase extends the lifespan of virus-transformed human cells without net telomere lengthening. *Proc Natl Acad Sci U S A* 96: 3723-8.